

REPORT DOCUMENTATION PAGE

0361

Public reporting burden for this collection of information is estimated to average 1 hour per response, including the time for reviewing instructions, searching existing data sources, gathering the required information, reviewing the collection of information, Send comments regarding this burden estimate or any other aspect of this collection of information, including suggestions for reducing the burden, to Washington, DC 20503. Send comments regarding this burden estimate or any other aspect of this collection of information, including suggestions for reducing the burden, to Washington, DC 20503. Send comments regarding this burden estimate or any other aspect of this collection of information, including suggestions for reducing the burden, to Washington, DC 20503.

1. AGENCY USE ONLY (Leave blank)		2. REPORT DATE 31 MARCH 1998		3. REPORT TYPE AND DATES COVERED FINAL REPORT 1 JUN 97 - 28 FEB 98	
4. TITLE AND SUBTITLE A VACUUM ARC ION THRUSTER FOR SPACE PROPULSION				5. FUNDING NUMBERS F49620-97-C-0024 3005/SS 65502F	
6. AUTHOR(S) NIANSHENG QI, STEVE GENSLER, RAHUL R. PRASAD, MAHADEVAN KRISHNAN, ALEKSEI VIZIR AND IAN BROWN					
7. PERFORMING ORGANIZATION NAME(S) AND ADDRESS(ES) ALAMEDA APPLIED SCIENCES CORPORATION 2235 POLVOROSA AVENUE, SUITE 230 SAN LEANDRO, CA 94577				8. PERFORMING ORGANIZATION REPORT NUMBER	
9. SPONSORING/MONITORING AGENCY NAME(S) AND ADDRESS(ES) AIR FORCE OFFICE OF SCIENTIFIC RESEARCH (AFOSR) 110 DUNCAN AVENUE SUITE B115 BOLLING AFB DC 20332-8050 NA				10. SPONSORING/MONITORING AGENCY REPORT NUMBER	
11. SUPPLEMENTARY NOTES					
12a. DISTRIBUTION AVAILABILITY STATEMENT APPROVED FOR PUBLIC RELEASE, DISTRIBUTION IS UNLIMITED				12b. DISTRIBUTION CODE	
13. ABSTRACT (Maximum 200 words) The Phase-I project has demonstrated the feasibility of a 500 W vacuum arc ion thruster (VAIT) that is very different from present Xe ion thrusters that are in production for space missions. The VAIT does not require storage and feed of gases, reducing the parts count considerably. The VAIT produces a highly ionized plasma with minimal neutral build-up in the grids, potentially making the grid lifetime longer and potentially allowing smaller grid spacing to be used. The VAIT has been shown (in related research over two decades) to produce plasmas (hence directed ion beams) of dozens of heavy ions such as Ba, La, Ce, Pr, Nd, Sm, Gd, L)y, Ho, Er, Tm, Yb, H(Ta, W, Ir, Pt, Au, Pb, Bi, Th and U. This wide range of possible ions provides great flexibility to the VAIT, allowing us to tailor different ion beams (with different thrust/specific impulse levels) to different missions. Ion streaming velocities of 5x104 m/s were measured using time-of-flight (TOF) methods, which imply a thrust level of 0.13 N.					
14. SUBJECT TERMS				15. NUMBER OF PAGES 35	
				16. PRICE CODE	
17. SECURITY CLASSIFICATION OF REPORT UNCLASSIFIED		18. SECURITY CLASSIFICATION OF THIS PAGE UNCLASSIFIED		19. SECURITY CLASSIFICATION OF ABSTRACT UNCLASSIFIED	
				20. LIMITATION OF ABSTRACT	

19980430 087

14 APR 1998

Report #aasc98TM-12

A Vacuum Arc Ion Thruster for Space Propulsion

SBIR Phase-I Final Report

Period of Performance: June 1, 1997 to Feb. 28, 1998

by

Niansheng Qi, Steve Gensler, Rahul R. Prasad and Mahadevan Krishnan

Alameda Applied Sciences Corporation
2235 Polvorosa Ave., Suite 230, San Leandro, CA 94577

and

Aleksei Vizir and Ian Brown

Lawrence Berkeley National Laboratory, *Berkeley, CA 94577*

submitted to

Dr. Mitat Birkan
(202) 767-4938
AFOSR/NA

Directorate of Aerospace and Materials Sciences
110 Duncan Ave., Room B115
Bolling AFB, DC 20332-8050

for

Contract # F49620-C-0024

March 31, 1998

DTIC QUALITY INSPECTED 3

1. Introduction

Alameda Applied Sciences Corporation (AASC) and its co-operative partner, the Plasma Application Group at Lawrence Berkeley National Laboratory (PAG/LBNL) were awarded this Phase I SBIR to explore development and commercialization of a sub-kW Vacuum Arc Ion Thruster (VAIT) for electric propulsion. The proposed VAIT thruster uses a solid propellant, which offers several advantages over gas discharge thrusters. The overall period of performance of the Phase I effort is from June 1, 1997 to February 28, 1998. By the end of December 1997, we had met all of the objectives for the Phase-I effort. The Phase-I feasibility studies have demonstrated that a properly designed vacuum arc ion thruster can produce an efficient ion beam for space propulsion.

Most ion thrusters use gases as a propellant. As the turn-on time is long, most of these thrusters are operated in DC mode. This has induced several short comings. At an optimum operating condition, the ion current level has a limited range for a given acceleration grid set. As the thrust is proportional to the ion current, it is not possible to adjust the thrust level without loss of efficiency. Therefore, it may not energy efficient to use this type of thruster for station keeping applications, where turn-on/turn-off operation and thrust level changes occur very often. Another major advance required for the ion thruster is to obtain necessary thruster lifetime of 5-20 years. Cathode erosion is a serious issue for the lifetime of the gas ion thruster. As the discharge plasma from the gas is partially ionized, charge exchange in the acceleration grids could enhance the erosion of the grids and reduce the lifetime of the system. Partially ionized gas also causes electric breakdown of the acceleration grids. Thus, the acceleration field is limited to ~ 2 kV/mm, which results low beam current density. Using gases as a propellant, storage and feed-in systems of the propellant are heavy and complicated. Sometimes, the spacecraft is designed for high vacuum (say 10^{-8} torr) operation. Small leakage of the gas propellant could spoil the vacuum and might cause system failure.

The above shortcomings of xenon or other gas ion thrusters can be avoided when a pulsed vacuum arc discharge source is used to replace the gas discharge system. The vacuum arc ion source [1-3] is a good candidate for an ion thruster. Ion beams of any of the solid metals of the periodic table [1,4], as well as metallic compounds and alloys can be produced. Time-of-flight measurements of the ion beam charge state composition have shown that the beam ions are predominantly of charge states $1+$ to $3+$ depending on the metal species used and the arc current density applied, with no significant impurity contamination. High current, low divergence heavy ion beams have been demonstrated with pulse widths from few μ s to few ms.[5,6] This implies that the thrust dynamic range of the vacuum arc ion thruster could be as high as 1000:1.

At an optimum operating condition of the ion thruster, there is a certain beam current level for a given acceleration grid set.[7,8] Various thrust levels are easily delivered from the vacuum arc ion thruster by adjusting the pulse width of the arc current or the repetition rate of the arc plasma without changing the ion current. As there are no permanent magnets needed for VAIT, there is no issue of the degaussing of the magnets due to excessive heating and the overall system mass is much lower. The plasma from the arc is fully ionized. Erosion of the acceleration grids due to charge exchange with neutrals is not an issue. As the arc cathode *itself* is the

AAC

propellant, there is no issue of cathode erosion. The spent cathode can be replaced by a simple mechanical feed. Using heavy metals such as Bi ($A=209$), the ion beam current is reduced (for a given thrust) by a factor of 40% as compared with a xenon gas propellant. The lifetime of the thruster could be much longer as it is roughly proportional to the beam current. Also, the acceleration electrical fields between the grids can be increased when using a fully ionized arc plasma and the beam current density is increased. Therefore, the aperture of the acceleration grids can be reduced to 20-40% to deliver the same thrust as from the xenon ion thrusters. These advantages, if proven fully in Phase-II, could lead to a compact, lower mass, long life vacuum arc ion thruster.

In summary, vacuum arc ion sources have several advantages over other, more conventional approaches:

- easy and rapid turn-on/turn off.
- simplicity of fabrication and operation.
- generation of a fully ionized plasma so that the erosion of the grids is reduced.
- cathode erosion is not a issue.
- production of heavy ion beams ($A > 200$) from metals to increase the thruster lifetime.
- storage and feeding of the propellant are simple.
- control of the thrust level is easily made by varying either the arc pulse width or the repetition rate.

AASC has proposed a three Phase technical approach for the VAIT development:

- The Phase-I effort would address the feasibility of the VAIT for space propulsion applications.
- The Phase-II effort would advance the research and development of the VAIT for the electric propulsion application, understand optimum operating parameters, construct and deliver a prototype VAIT to Phillips Lab. for rigorous testing after the Phase-II project.
- Following successful development in Phase-II, the Phase-III effort would commercialize the vacuum arc ion thruster and supply the thrusters to the government for the electric propulsion application as well as modify the thruster for other commercial applications.

The key Milestones for the three Phase program identified at the start were:

1. Demonstrate that the VAIT is comparable in energy efficiency to present xenon ion thrusters. (Phase-I)

2. Exploit the flexibility of the VAIT by studying different elements from a myriad of candidates (Ba, La, Ce, Pr, Nd, Sm, Gd, Dy, Ho, Er, Tm, Yb, Hf, Ta, W, Ir, Pt, Au, Pb, Bi, Th and U) to find the optimum materials as a propellant. (Phase-II)
3. Perform engineering optimization of the arc plasma profile and electrode geometry; study erosion rates for lifetime evaluation, quantify the potential limitations of the VAIT such as spacecraft contamination by the high-Z materials used and establish optimum operating parameters for practical thrusters. (Phase-II)
4. Design, fabricate and assemble a prototype VAIT for delivery to Phillips Lab. (Phase-II)
5. Assist Phillips Lab. with establishment of performance and lifetime limits for the VAIT. (Phase-III)
6. Pursue commercial spin-offs of the VAIT technology such as new ion beams for materials modification, better heavy ion sources for Heavy Ion Fusion Injectors and exotic ion beams for nuclear research. (Phase-III)

The Phase-I project has achieved the first of these milestones. We have demonstrated that this vacuum arc ion thruster can produce $\approx 1.3 \text{ A/3 kV Bi}$ ion beams with $\approx 12 \text{ cm}$ diameter acceleration grids. Ion streaming velocities of $5 \times 10^4 \text{ m/s}$ were measured using time-of-flight (TOF) methods, which imply a thrust level of 0.13 N . The goals of the Phase-I project were to produce a beam with an energy efficiency (defined as beam energy/(beam energy + arc energy)), of $\approx 80\%$ and a divergence angle of $\leq 0.1 \text{ rads}$. Both goals have been achieved. The ion current is about 2.2% of the arc current for an extraction voltage of 3 kV . The discharge power is 900 W while the extraction grid power is 3900 W . If such a system is operated at a duty factor of 10% , the average power (discharge + grids) would be 480 W . The Phase-I project has demonstrated the feasibility of a 500 W vacuum arc ion thruster (VAIT) that is very different from present Xe ion thrusters that are in production for space missions. The VAIT does not require storage and feed of gases, reducing the parts count considerably. The VAIT produces a highly ionized plasma with minimal neutral build-up in the grids, potentially making the grid lifetime longer and potentially allowing smaller grid spacing to be used. The VAIT has been shown (in related research over two decades) to produce plasmas (hence directed ion beams) of dozens of heavy ions such as Ba, La, Ce, Pr, Nd, Sm, Gd, Dy, Ho, Er, Tm, Yb, Hf, Ta, W, Ir, Pt, Au, Pb, Bi, Th and U. This wide range of possible ions provides great flexibility to the VAIT, allowing us to tailor different ion beams (with different thrust/specific impulse levels) to different missions.

The rest of this report is arranged as follows: Section 3 describes the experimental apparatus. Section 4 presents the results of the experiments and Section 5 discusses their implications.

2. Principle and Description of the Vacuum Arc Ion Source

2.1. Background of the Vacuum Arc Ion Source

High current beams of metal ions can be produced by using the dense and highly ionized metal plasma that is generated by a vacuum arc. Ion production in the vacuum arc has been investigated at a fundamental level over the past several decades by a number of authors.[9-12]

AC

Early attempts to incorporate the arc as the method of plasma production in an ion source were made as part of the Manhattan Project in World War II.[13] More recently ion sources of this kind have been investigated by a growing number of research groups from many different laboratories [14,15] including LBNL, as described here.

The vacuum arc ion source provides a simple and straightforward way of producing very high current beams of metal ions. A vacuum arc plasma source is appropriately located with respect to a set of beam formation electrodes ("extractor grids") in a vacuum housing. Metal plasma is produced by a vacuum arc discharge from a macroscopically cold cathode. The plasma production mechanism is neither by evaporation nor sputtering, and no oven nor background gas is required. The metal plasma plume produced at cathode spots [16,17] in a manner reminiscent of laser plasma production, streams toward the extractor where the ion separation and acceleration are performed. Typically a multi-aperture, triple grid extractor (plasma grid, electron suppressor grid, and ground grid) is used. The ion beam that is formed can be narrow or broad depending on the intended application, varying from a few millimeters in diameter up to tens of centimeters, with ion energy in the range of a few keV up to several hundred keV, and with pulsed ion current up to many amperes. Pulse lengths can be from a few microseconds upwards, and the pulse repetition rate can readily be up to a few hundred pulses per second (for short pulse duration).

The main applications for which this kind of ion source have been used are ion implantation and accelerator injection. In the accelerator injection application, for example, the source is unsurpassed in terms of the beam current of Uranium and other heavy metal ion beams that it can provide for injection into heavy ion synchrotrons. In the space propulsion application, the vacuum arc source has several advantages over the gas source. This area has not been investigated widely. This Phase I has provided us a good opportunity to carry out such an investigation.

2.2. Description of the experimental apparatus

The major Phase I experiments were performed at the PAG/LBNL facility, jointly by AASC and the PAG/LBNL. A modified vacuum arc ion source that previously made at PAG/LBNL was used to accomplish the Phase I objectives.

Figure 1 shows the existing vacuum arc ion source. In the past, we have used this ion source for Heavy Ion Fusion (HIF) studies, where ~2 cm diameter, $\approx 20 \mu\text{s}$, $\sim 0.1 \text{ A}$, $\approx 120 \text{ keV}$, Gd ion beams have been produced with an arc current of $\approx 300 \text{ A}$. For space propulsion applications, it is desired to produce a long pulse ($\geq 200 \mu\text{s}$), high beam current ($\sim 1 \text{ A}$), low energy (1-5 kV) heavy ion beam with a low arc current. To meet these requirements, we have designed and fabricated pulse forming networks to produce arc plasmas with either a $\approx 250 \mu\text{s}$ or a $\approx 2 \text{ ms}$ current pulse width, new anode/cathode configurations for the arc plasma and several sets of large diameter acceleration grids for ion extraction.

The ion source at LBNL was modified for this project. Several beam extraction grids were designed and fabricated. An eight stage LC pulse forming network was used to generate a 10-

100A arc discharge with a $\approx 250 \mu\text{s}$ flat top pulse width. The goal of this task was to produce $\sim 1 \text{ A}/250 \mu\text{s}$ heavy ion beams with specific impulse of $\approx 5000 \text{ s}$ and has been achieved.

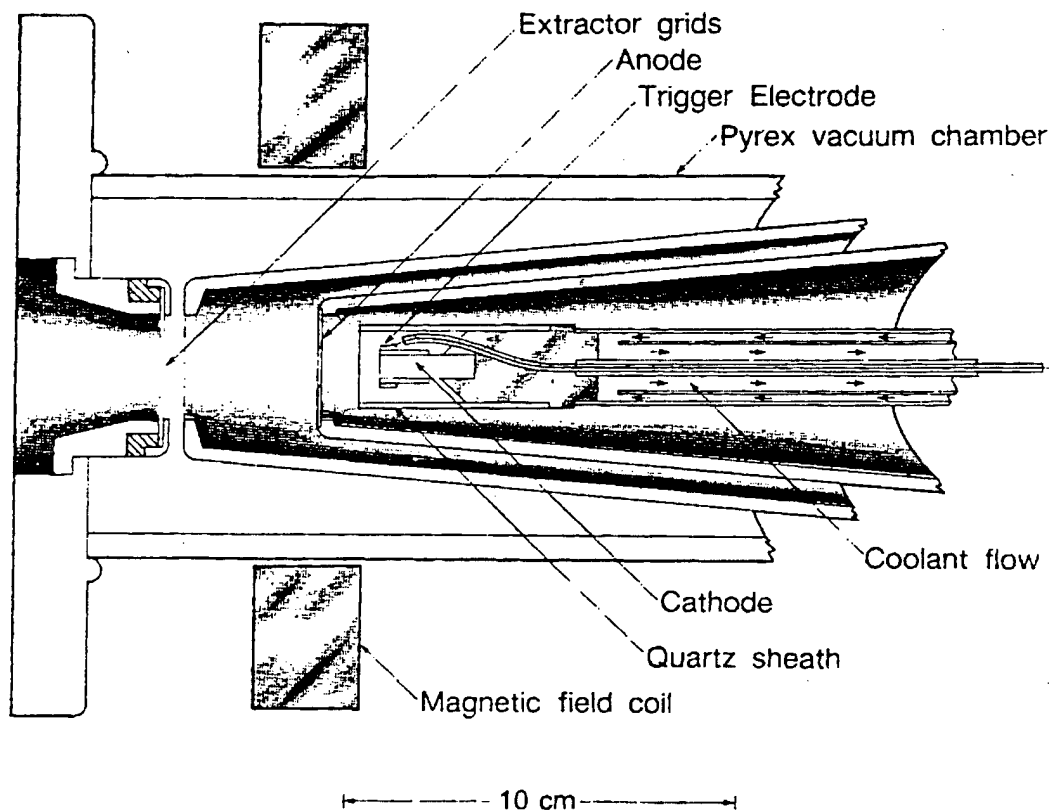


Figure 1 Drawing of the existing vacuum arc ion source at LBNL. The source consists of an arc plasma generator (cathode/anode/trigger combination, forming "the plasma gun") and a set of extractor grids. Plasma formed at the cathode plumes through the annular anode toward the extractor grids, where ion separation and acceleration occur.

Figure 2 shows a modified ion source for VAIT development. Metal plasma formed at the cathode plumes toward the extractor grids, where ion separation and acceleration occur. A high current beam of metal ions is produced and exits through the grounded final extractor grid. The grids used were 0.25 mm thick, 64% transparency W meshes. The cathode was 6.25 mm in diameter and was extended from the base to deliver more plasma to the extraction grids. The beam acceleration system consisted of three (or two) grids with $\approx 70\%$ open area. The space between the grids was $\approx 1.6 \text{ mm}$. It was designed to first accelerate the ions to $\sim 4 \text{ kV}$ and then decelerate them to $\approx 3 \text{ keV}$. This accel-decel concept serves to capture electrons as well as to collimate the ion beam.

The distance from the cathode to the first acceleration grid is $\approx 5 \text{ cm}$. The discharge plasma expands from the cathode and fills an aperture larger than the grid diameter. At typical plasma densities, the Debye length is much smaller than the grid aperture size. This means that a meniscus will form at each grid aperture, from which individual ion beamlets will be extracted. The ion beam dynamics are not easy to calculate in this regime, requiring complex numerical codes.

AC

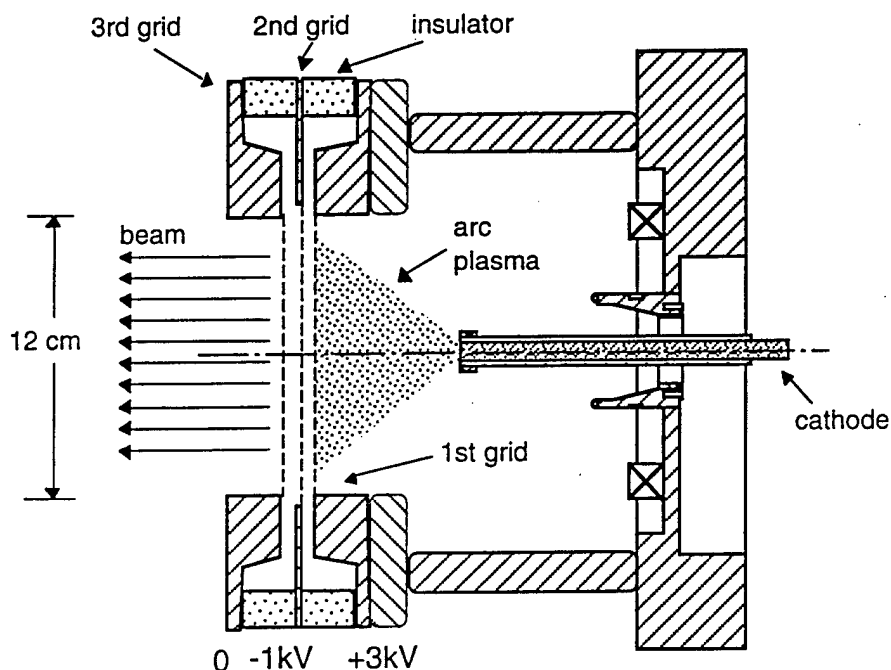


Figure 2 Schematic drawing of the VAIT: the VAIT consists of an arc plasma generator (cathode/anode/trigger combination, forming "the plasma gun") and a set of the extractor grids.

The electrical system to drive the ion source is shown in Fig. 3. The arc trigger pulse was approximately 10 kV in amplitude and few μ s in duration. It was delivered across the cathode, to induce a cathode-anode breakdown, by a step-up transformer which also served as high voltage isolation. The arc current was supplied by a Pulse Forming Network (PFN). The ion acceleration/extraction system consisted of two (not shown) or three-grid. Typical net acceleration voltage was +3 kV with a -1 kV electron suppresser as indicated in Fig. 2. This LBNL vacuum arc ion source was used for ion implantation studies and the whole ion source was floated at the +3 kV. The electrical system efficiency of the source was not very high since it was designed for the ion implantation applications, where the efficiency was not a serious issue. Because the required VAIT electrical system are very similar to that of the existing power supplies for the xenon gas ion thruster, it is easy to integrate these system into the VAIT. With the limited budget, the Phase I efforts were concentrated on the determination of the power (or energy) delivered into the arc discharge and of the extracted beam. This was accomplished by measuring the arc current and voltage, the acceleration voltage and the total ion beam current. As shown in Fig. 3, the arc current was measured by using a Pearson Transform. The arc discharge and the net beam acceleration voltages were monitored through a high voltage probe.

The beam characterization systems are shown in Fig. 4. A magnetically suppressed Faraday cup with a 5 cm diameter entrance aperture, located downstream of the extraction grids, was inserted into the beam path to measure the beam current. Scanning the Faraday cup along the radial direction gave the ion current profiles. The total ion beam current was derived by integrating the measured current profiles. The beam composition (charge to mass ratio of the ion components, Q/A) was obtained by means of a time-of-flight charge state diagnostic.[18] A sub-

microsecond sample of the beam pulse was gated on and the time of flight through a drift region of ≈ 103 cm was measured. Since the ions with different charge states traveled at different speeds, they were well separated after pass the meter long drift region. The TOF measurements also gave the ion energies.

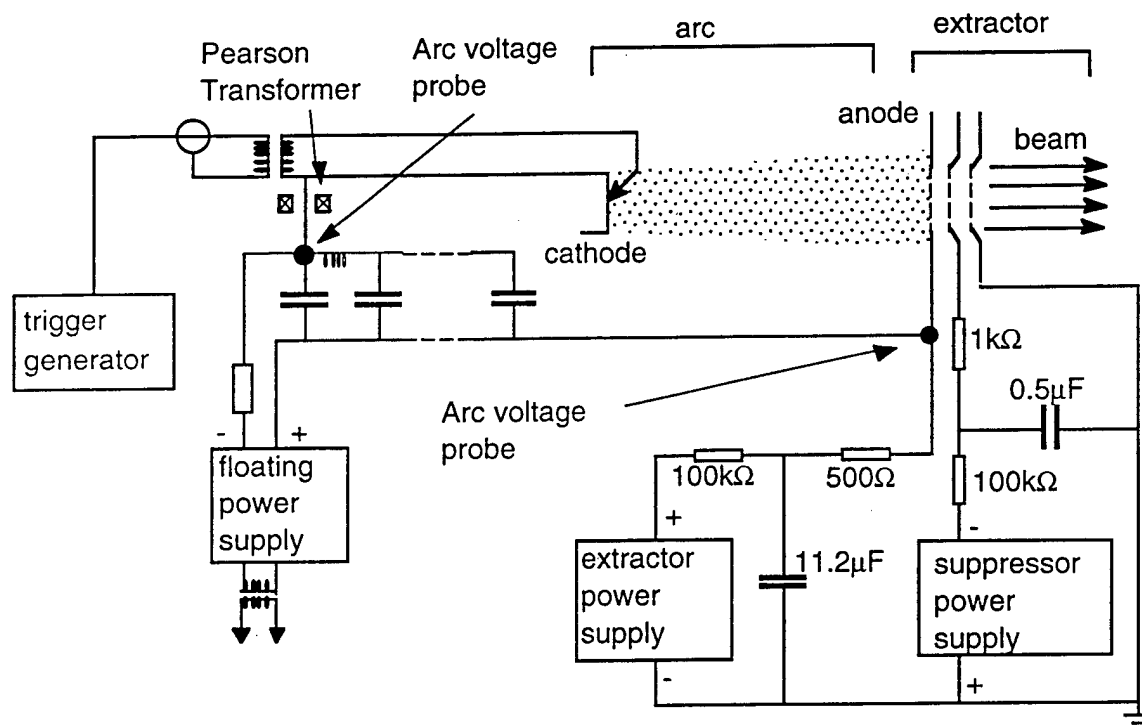


Figure 3 Schematic of the overall electrical circuit used for the vacuum arc ion source.

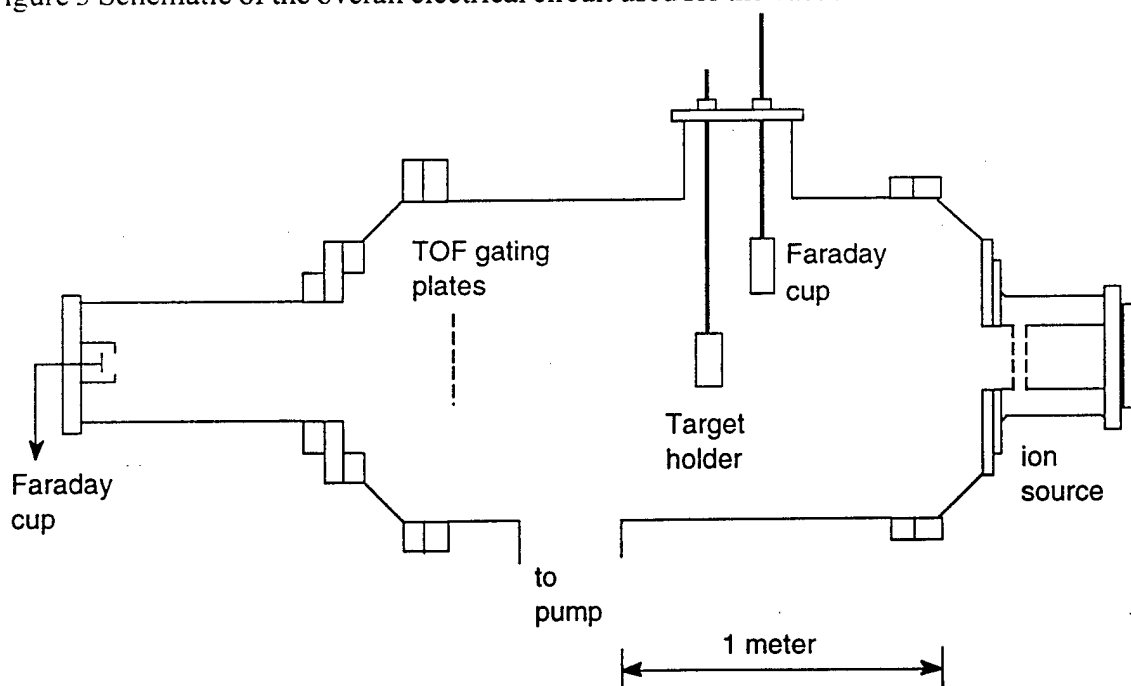


Figure 4 Experimental apparatus used at LBNL.

Results from the proof-of-principle experiments are presented in next section.

3. Experimental Results

3.1 Arc discharge characterization

Two multi-stage Pulse Forming Networks (PFN), which can deliver either a $\approx 250 \mu\text{s}$ or a $\approx 2 \text{ ms}$ arc current pulse, have been assembled. The cathode was biased at a negative voltage and was triggered by applying a high voltage pulse to the trigger ring. Figures 5 and 6 show the arc current and voltage traces from the 5 stage, 2 ms PFN and the 8 stage, 250 μs PFN, respectively. The cathode used was Bi. Using the 2 ms PFN, the cathode voltage was about -49 V before the discharge. During the discharge, the cathode voltage was between 13 and 15 V and the arc current was about 70 A. From the 250 μs PFN, the cathode voltage was about -100 V before the discharge. During the discharge, the cathode voltage was about 17 V and the arc current was about 60 A. It seems that the arc voltage drop from the 2 ms PFN is less than that from the 250 μs PFN for a given discharge current. It is possible that the 2 ms PFN might be more efficient to produce arc plasmas. However, since an arc current pulse with a more or less flat top will make the data analysis easier, the 250 μs PFN was used for the rest of the experiments. We will investigate the arc driver in future.

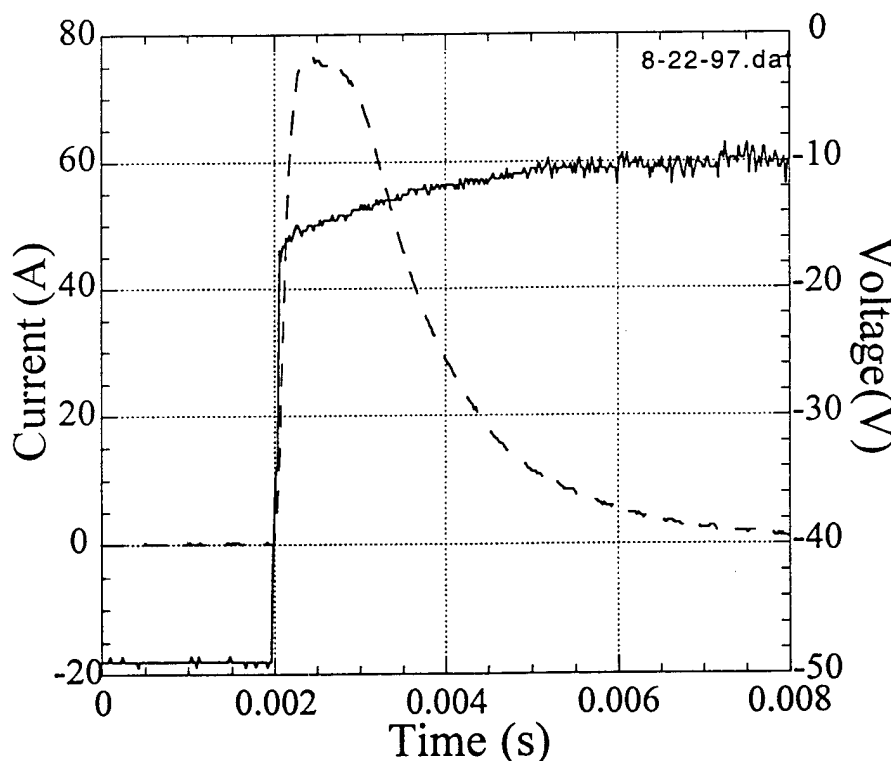


Figure 5 Current pulse (dashed line) and cathode voltage drop (solid line) from an 8 stage, $\sim 2 \text{ ms}$ pulse forming network with a Bi cathode.

The Bi arc voltage drop was measured with arc current range from 10 to 100 A using the 250 μ s PFN. As the current pulses were not perfect flat, we use the average current from each pulse as derived by integrating the current waveform and then dividing by the 250 μ s pulse width. The dashed horizontal line shown in Fig. 6 represents this calculated average arc current. The mean arc voltage, also shown in Fig. 6 as dashed horizontal line, was obtained by averaging the voltage pulse in the duration, where the arc current is higher than 90% of its mean value. Figure 7 shows the measured arc voltage and the estimated arc resistance. The arc voltage is almost linear with the current. To derive the arc resistance, a cathode voltage drop of 10.8 V was assumed. The arc resistance were ≈ 120 m Ω . From the calculated mean arc current and voltage values, the average arc discharge powers are derived as shown in Fig. 8. Integrating the product of the current and voltage pulse over time, the energy in each pulse is obtained, which is also shown in Fig. 8. The arc power (or energy per pulse) is proportional to the square of the arc current, as expected since the voltage is proportional to the current. The fitting formula for the arc energy is,

$$\text{Energy (J)} = 4.79 \times 10^{-4} + 2.59 \times 10^{-3} I + 3.96 \times 10^{-5} I^2 \quad (1)$$

where I is the arc current in amperes. The experiments indicated that the arc was stable at currents ≥ 10 A with a voltage drop of just tens of volts. This implies the arc discharge could be an efficient source of ions.

This is the first milestone that we have achieved in the Phase-I project.

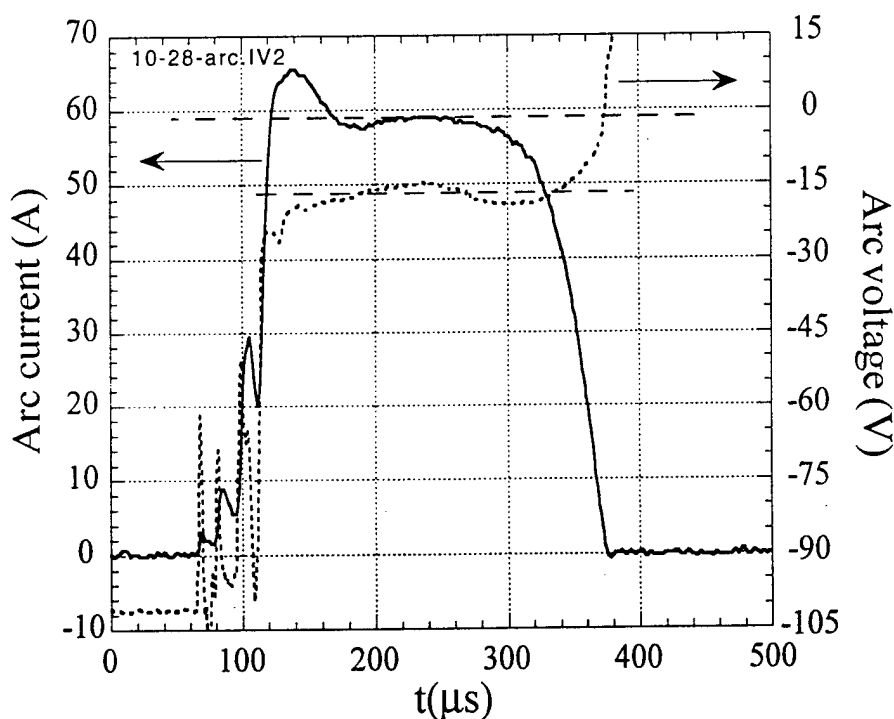


Figure 6 Current pulse (solid line) and cathode voltage drop (dashed line) from an 8 stage, ≈ 250 μ s pulse forming network with a Bi cathode. The dashed horizontal lines represent the average current and voltage of the arc.

AC

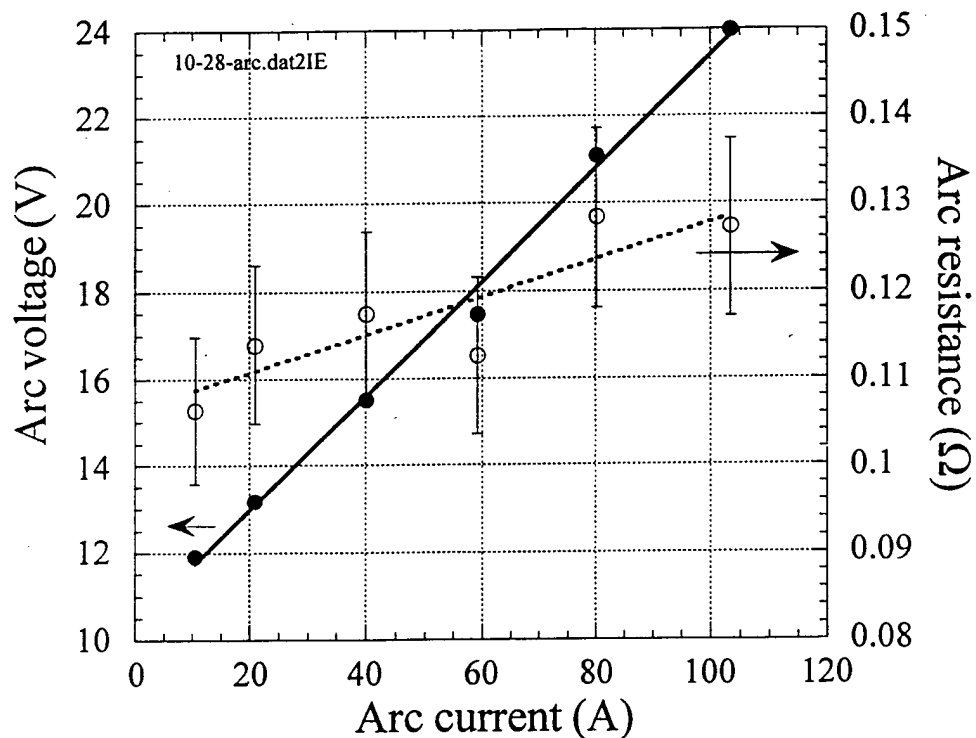


Figure 7 Measured Bi arc discharge voltage drop (solid dots) and the derived arc resistance (open circles) as a function of arc current. The arc resistance was about 120 mΩ.

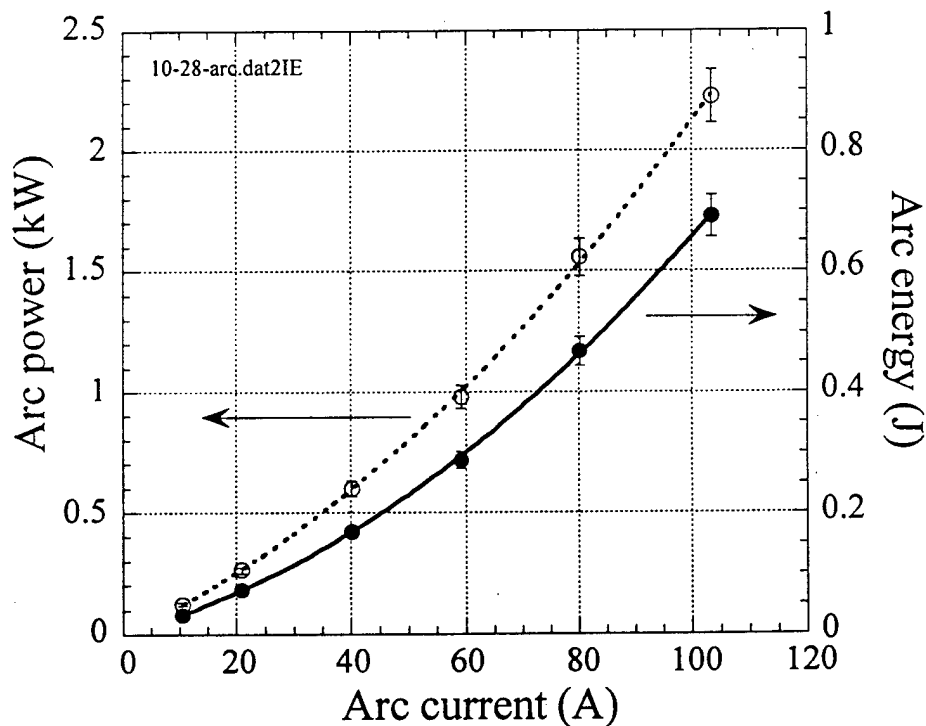


Figure 8 Measured average power (open circles) and energy (solid dots) of the Bi arc discharge as a function of the arc current.

3.2 Ion beam characterization

The 250 μ s PFN and a 5 mm diameter Bi cathode were used for creating the arc discharge in the beam extraction/characterization experiments. Acceleration systems with two and three-grid were tested in the experiments. Beam charge ionization states and beam profiles were measured. From these measurements, the divergence of the beam, the thrust level and the energy efficiency were derived.

3.2.1 Bi ion charge states measurements

The charge states of the ion beams were obtained using a time-of-flight device, where the ion streaming velocity can also be derived. A sub-microsecond sample of the beam pulse was gated on and the time of flight through a drift region of ≈ 103 cm was measured. Figure 9 shows the typical arc and beam current waveforms. There were ~ 25 μ s delay time between the arc current pulse and the downstream Faraday cup. Figures 10 a) or b) show the Bi ion charge states with an average net acceleration voltage of 3 or 2 kV sampled at several delay time respect to the beginning of the arc current. There is a ≈ 50 μ s propagation delay to the time-of-flight device. Thus, a 100 μ s delay time (in Fig. 10) is corresponding to 50 μ s after the beginning of the arc current. As shown in Fig. 10, at 2 (or 3) kV acceleration voltage, it took $1+$ Bi ions ≈ 24 (or ≈ 19.5) μ s to reach the end of the 103 cm long drift region, where the ions were collected by a Faraday cup. The measured ion velocity is consistent with the acceleration voltage. At 3 kV acceleration voltage, almost all of the ions had the same velocity, except at the late time of the current pulse. There were slightly variation in the ion energy with a 2 kV acceleration voltage. This could be due to the collision energy loss of the ions with the back ground gas. As shown in Fig. 10, ≥ 90 % ions were singly ionized and it is clear that the charge states of the beam are determined by the arc plasma production, not the acceleration voltage. To make an efficient beam high acceleration voltage is preferred so that the ratio of the beam energy is much higher than the arc energy. For space propulsion applications, there is an upper limit of the ion velocity. Therefore, it is desired to produce beams with most ions being in charge state of $1+$. The results of the charge state measurements is very encourage.

This is the second milestone we have achieved in Phase I.

3.2.2 Results from the three-grid acceleration system

The three-grid acceleration system as shown in Fig. 2 was used. The spacing between the 1st and the 2nd grids was 1.6 mm and between the 2nd and the 3rd was 2 mm. The beam profile and divergence as a function of the arc discharge current were measured by scanning a Faraday Cup over the beam radius. Figures 11a-11d show the measured beam current at several arc discharge current levels when the center of the 5 cm diameter Faraday cup was located at $R=0$, 2.5, ..., and 25 cm, respectively. In this case, a planar three-grid system was used. The beam current density was about few mA/cm² with a ≈ 1.6 mm gap between the grids. For such Bi ion beam current density at 3 keV ion energy, the ion source had to be operated at a $\geq 10^{-4}$ torr vacuum pressure so that the beam could be neutralized with the background pressure and

AC

propagate downstream. At large radius (for example, $R > 12$ cm with 60 A discharge current), there was a sharp peak in the early time of the beam current pulses. This is due to the space charge blow up of the beam and it disappeared in the later portion of the pulse since the beam was neutralized through the collisions. At low arc current level (~ 30 A, see Fig. 11d), ion current pulse was not flat due to the lack of sufficient supply of the ions from the arc plasma. At a ~ 80 A arc discharge, the plasma density near the acceleration grids matched the perveance condition and the ion beam pulse was flat (see Figs. 11b and 11c at $R=0$). At higher arc current (≥ 100 A), optimum conditions were matched at the rise and fall part of the arc current and there was a dip in the beam current pulses as shown in Fig. 11a ($R=0$). The diameter of the beam, measured 74 cm downstream of the extraction grids, was about 20 cm at arc current level of ≤ 80 A. Since the aperture of the acceleration grids was about 10 cm in diameter, the beam divergence is estimated to be ≤ 50 mrad. At high arc discharge currents (≥ 100 A), the beam diameter was less than 10 cm. This effect is due to the plasma sheath structure, which modifies the effective geometry of the acceleration grids.[8]

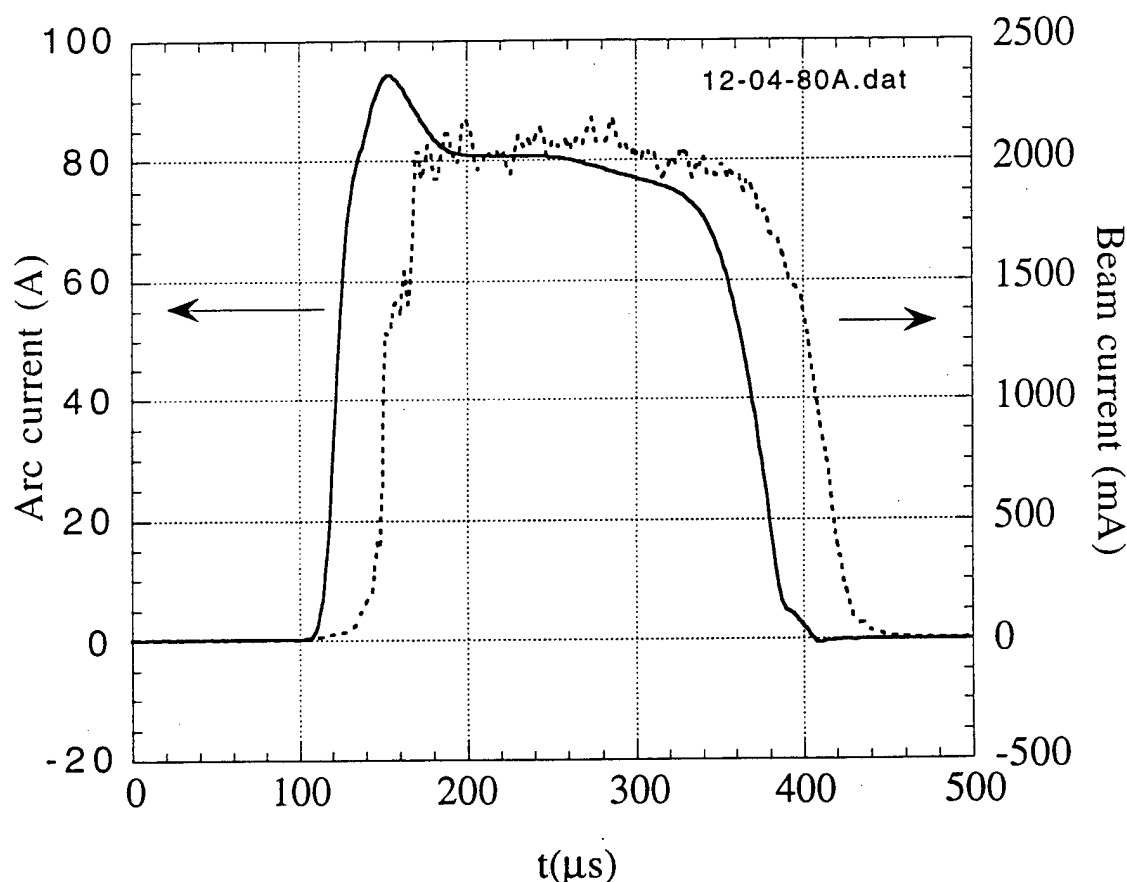


Figure 9 Typical Bi arc discharge current (solid line) and total beam current (dotted line) waveforms.

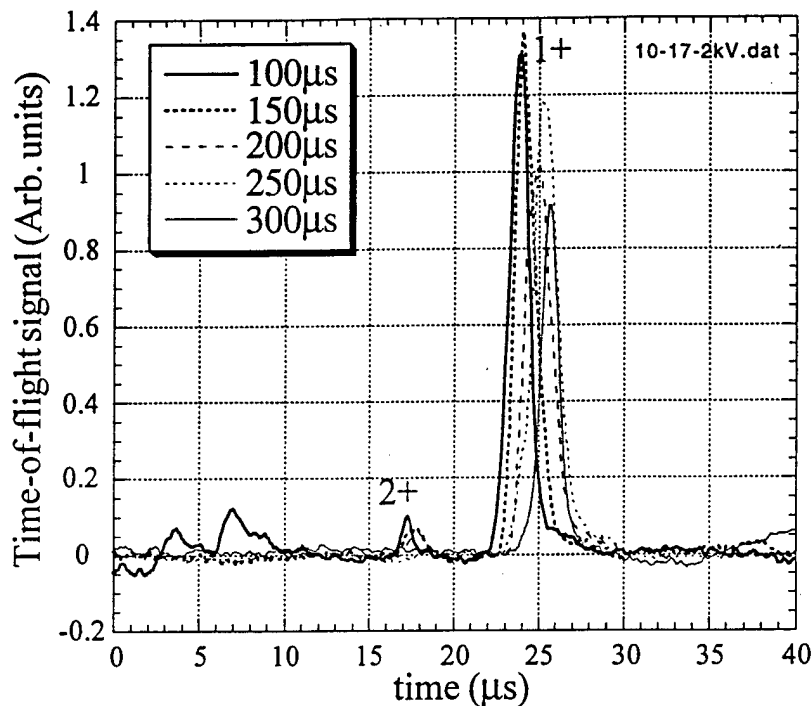


Figure 10a. Measured Bi ion charge states with an extraction voltage of 2 kV sampled at several portions of the beam pulse. The sub-microsecond gate pulse (not shown) of the time-of-flight device was at $t=0$. The $1+$ ion streaming velocity was about $4.3 \text{ cm}/\mu\text{s}$.

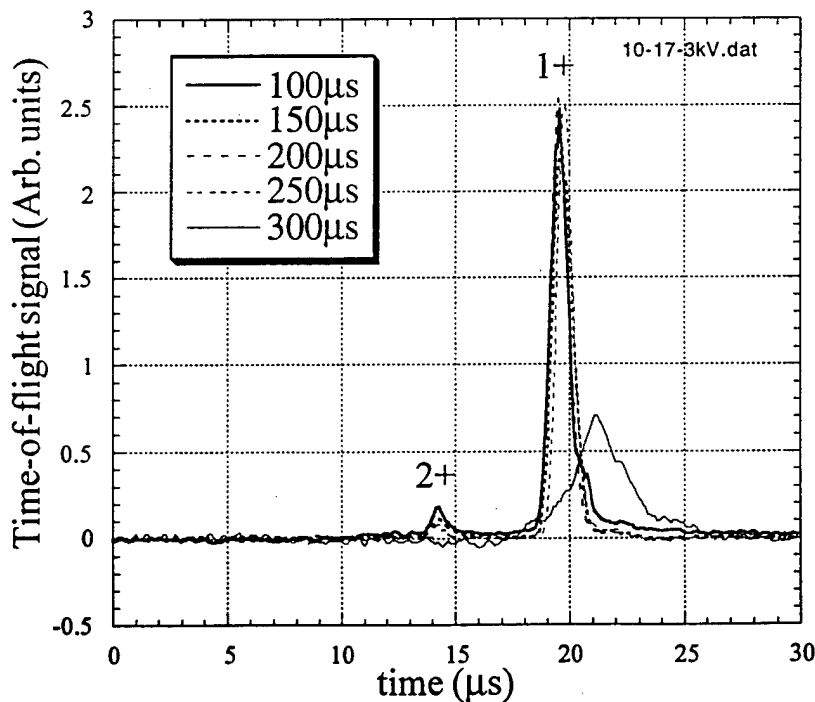


Figure 10b Measured Bi ion charge states with an extraction voltage of 3 kV sampled at several portions of the beam pulse. The sub-microsecond gate pulse (not shown) of the time-of-flight device was at $t=0$. The $1+$ ion velocity was about $5 \text{ cm}/\mu\text{s}$.

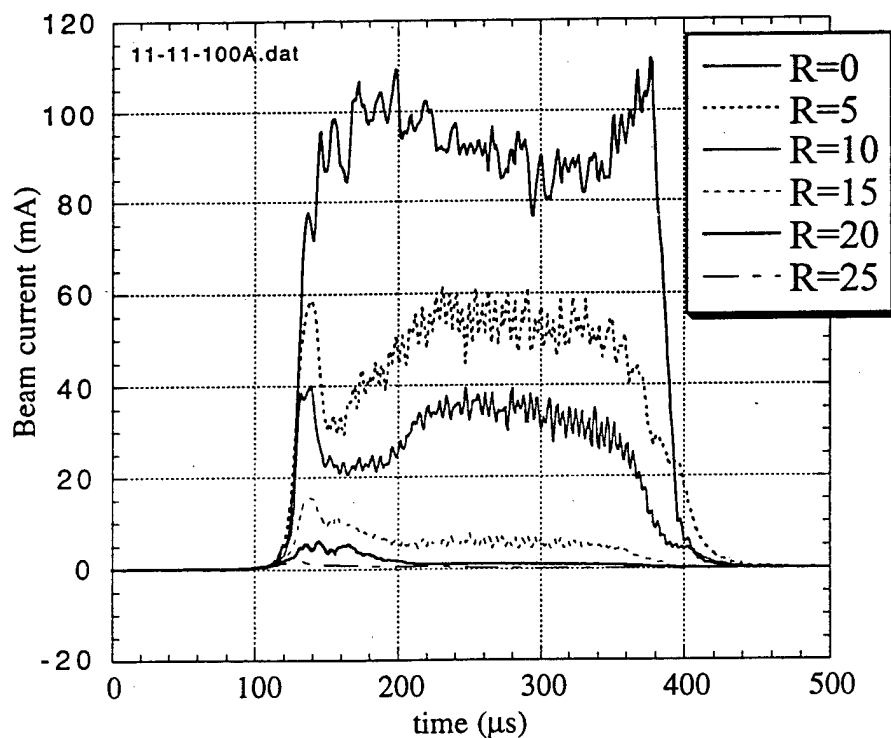


Figure 11a Measured Bi ion beam current at several radial positions with a 100 A arc discharge. The beam diameter was less than 10 cm.

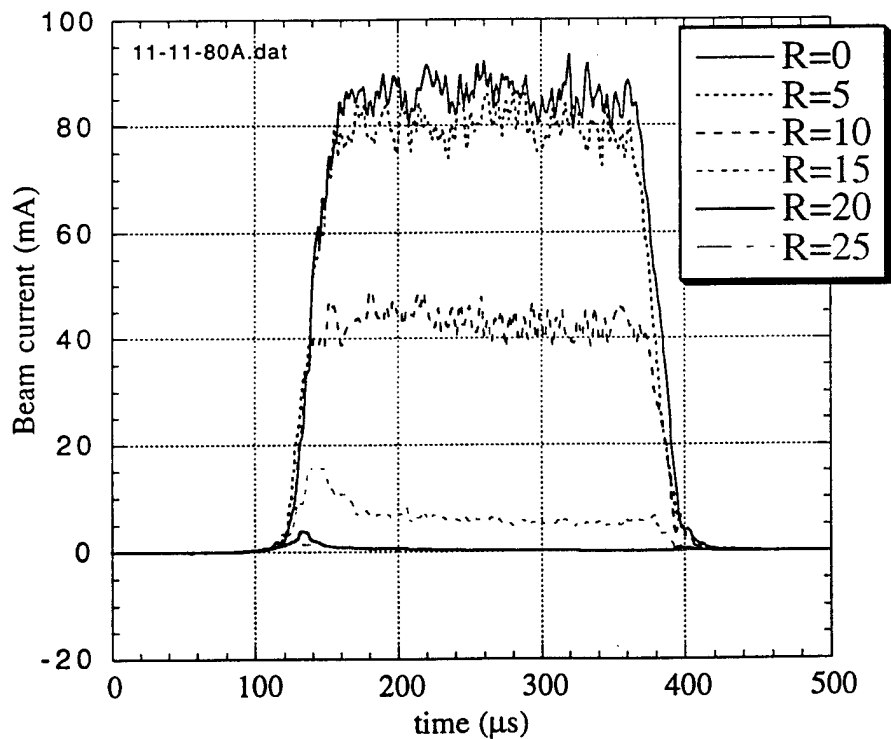


Figure 11b Measured Bi ion beam current at several radial positions with a 80 A arc discharge. The beam diameter was ≈ 10 cm.

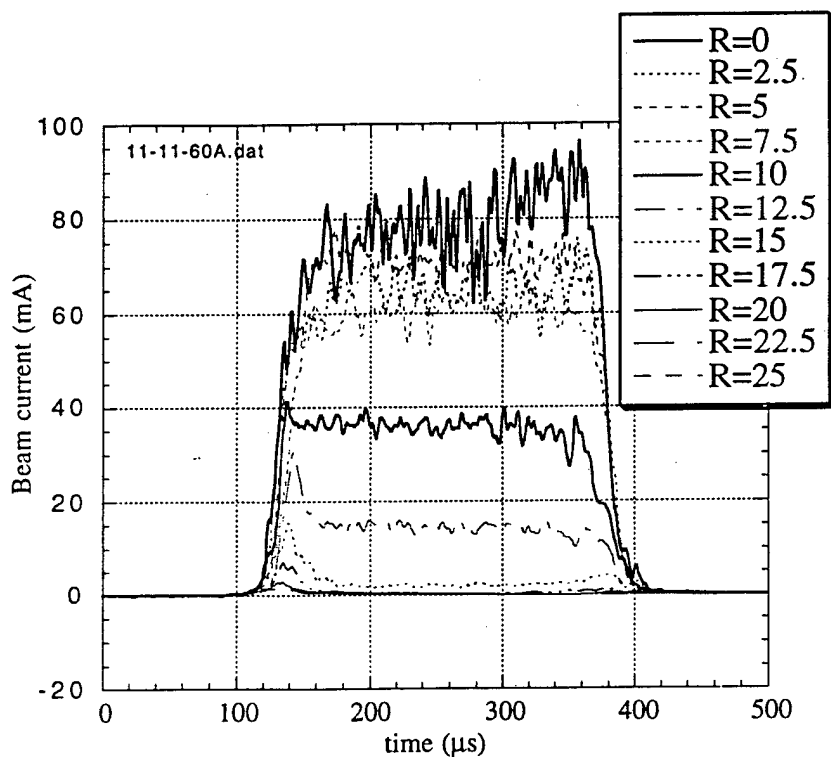


Figure 11c Measured Bi ion beam current at several radial positions with a 60 A arc discharge. The beam diameter was ≈ 10 cm.

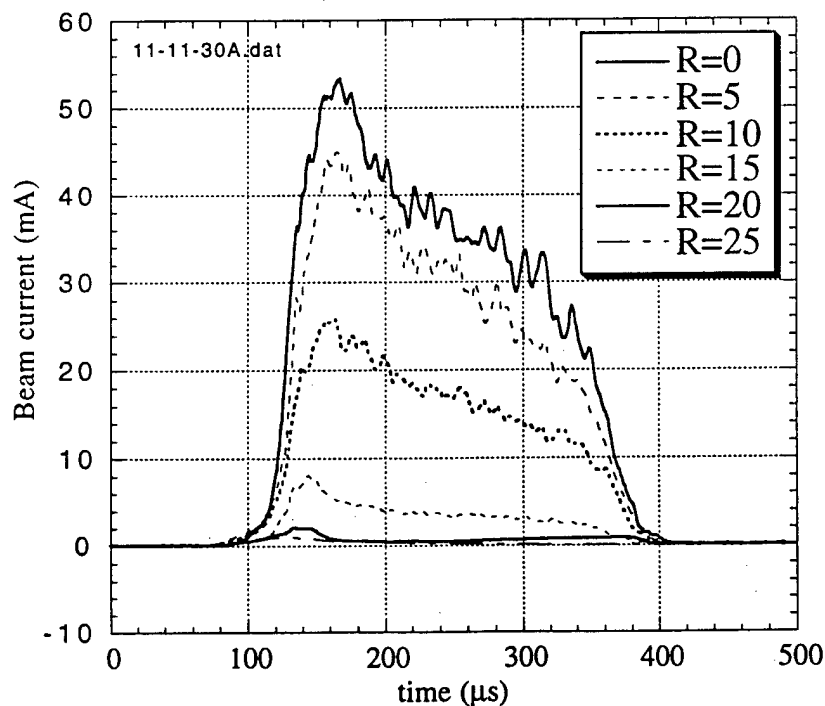


Figure 11d Measured Bi ion beam current at several radial positions with a 30 A arc discharge. The beam diameter was ≈ 10 cm.

AC

The total beam current was obtained by integrating the measured beam profile. Figures 12a-12d show the total ion beam current and the corresponding arc current. It took about 25 μs for ions to propagate downstream to the Faraday cup. At arc current levels of 60-80 A, the arc and beam pulses were very similar. At higher or lower arc current levels, there was no flat portion in the beam current waveforms. For the ion current pulses which were not perfectly flat, we calculate the average current from each pulse by integrating the current waveform and then dividing by the 250 μs pulse width as we did to obtain the average arc currents. The dashed horizontal line shown in Figs. 12 represents this calculated average ion current. Figure 13 shows the measured ion beam current as a function of the arc current. Also, shown is the ratio of the beam to the arc currents. It is clear that this ratio is high at low arc currents, which means higher efficiency with lower arc current. But the beam extraction is strongly dependent on the geometry of the grids. This ratio could be increased at higher arc current levels by using optimized extraction grids. In the future Phase-II work, we hope to explore this issue.

Figures 14a-14d show the waveforms of the ion beam current and the net acceleration voltage. The acceleration voltage was provided from a charged 11.2 μF capacitor, which was connected in series with an external 500 Ω resistor and the ion beam load. The net acceleration voltage pulse, shown in Figs. 14, was measured at the acceleration grid with respect to the ground (see Fig. 3). Initially, the acceleration voltage was equal to the charging voltage of the capacitor since the load resistance was infinity. With the arc plasma, ion beams were extracted from the grids. The acceleration voltage was reduced since there was a voltage drop on the 500 Ω external resistor. Such voltage drops could give an estimation of the beam current. For arc current levels of 60-80A, the calculated beam current from the acceleration voltage drop agrees with that measured by the Faraday cup as shown in Fig. 14c.

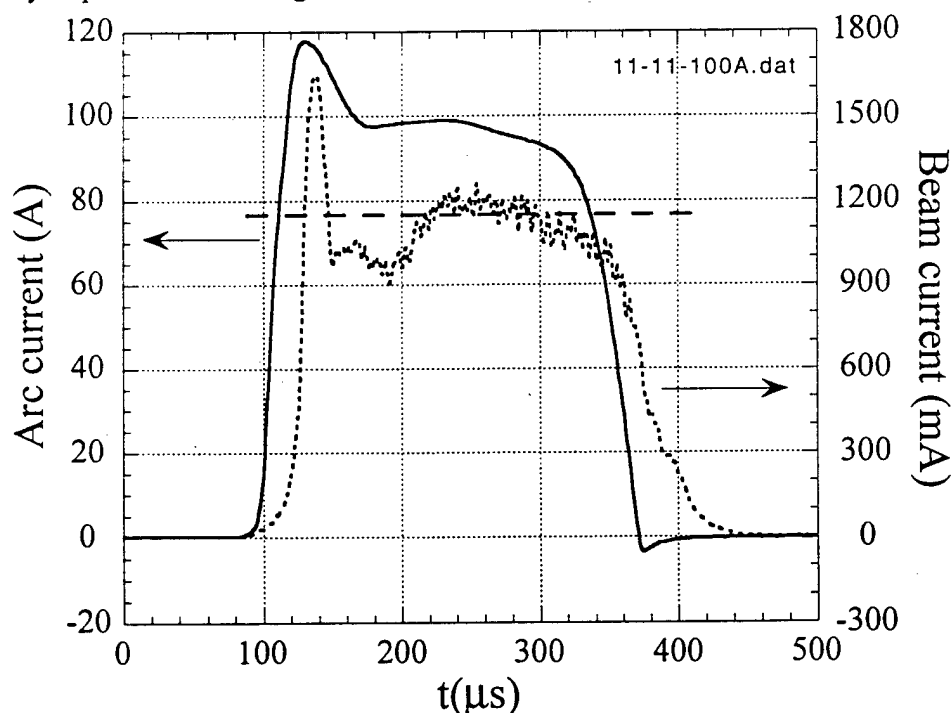


Figure 12a Bi arc discharge current (solid line) and total beam current (dotted line) vs. time.

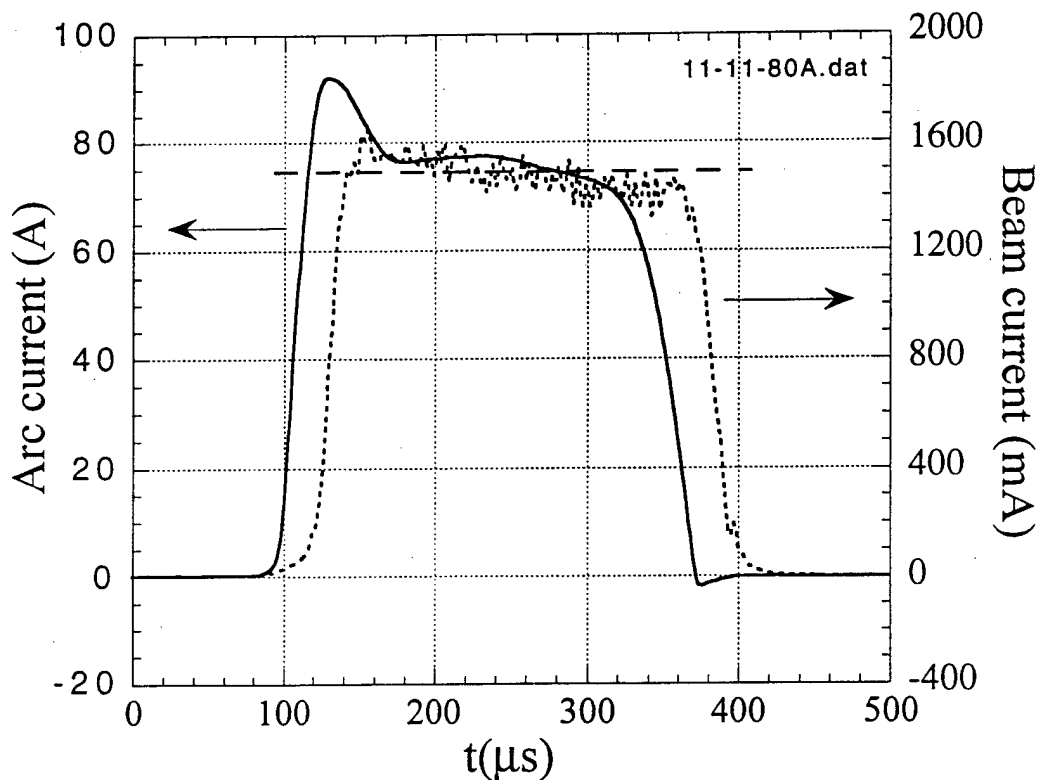


Figure 12b Bi arc discharge current (solid line) and total beam current (dotted line) vs. time.

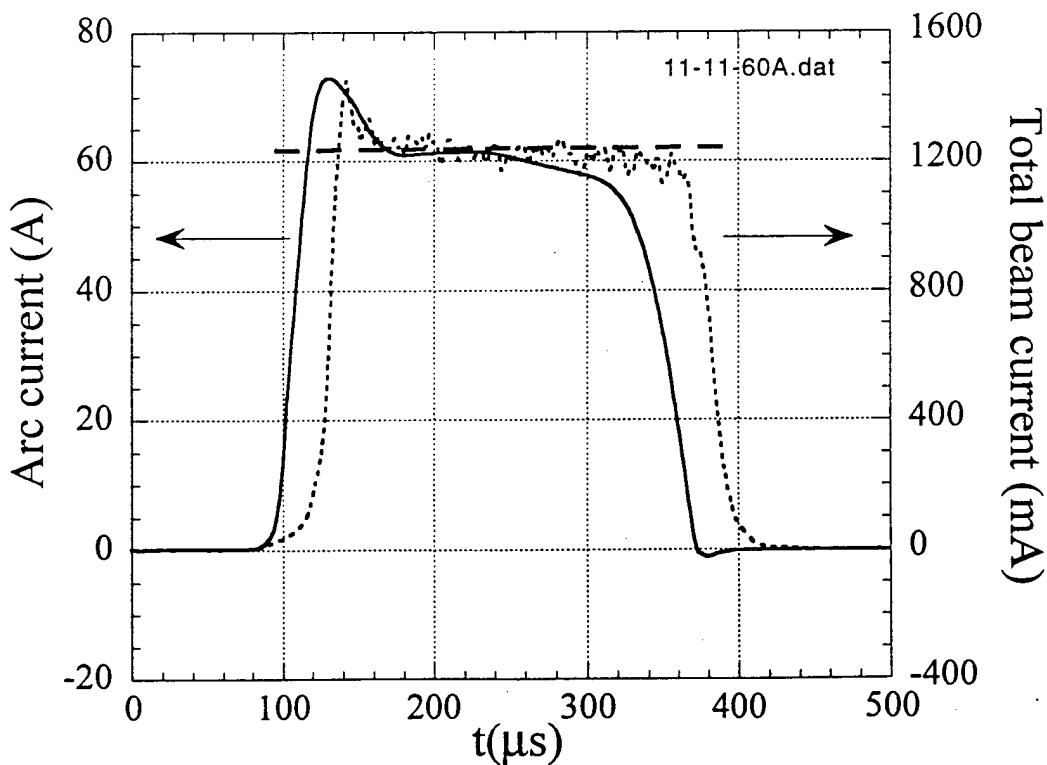


Figure 12c Bi arc discharge current (solid line) and total beam current (dotted line) vs. time.

AC

Use or disclosure of the proposal data on lines specifically identified by underlined text are subject to the restriction on the cover page of this proposal.

ALAMEDA APPLIED SCIENCES CORPORATION

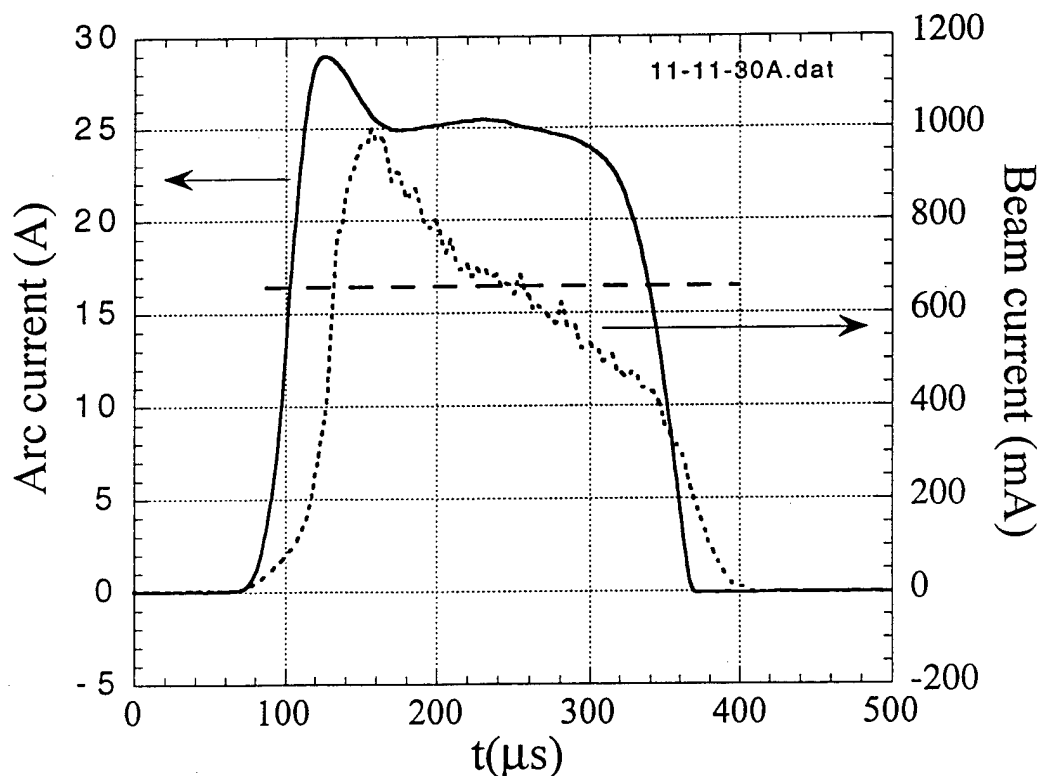


Figure 12d Bi arc discharge current (solid line) and total beam current (dotted line) vs. time.

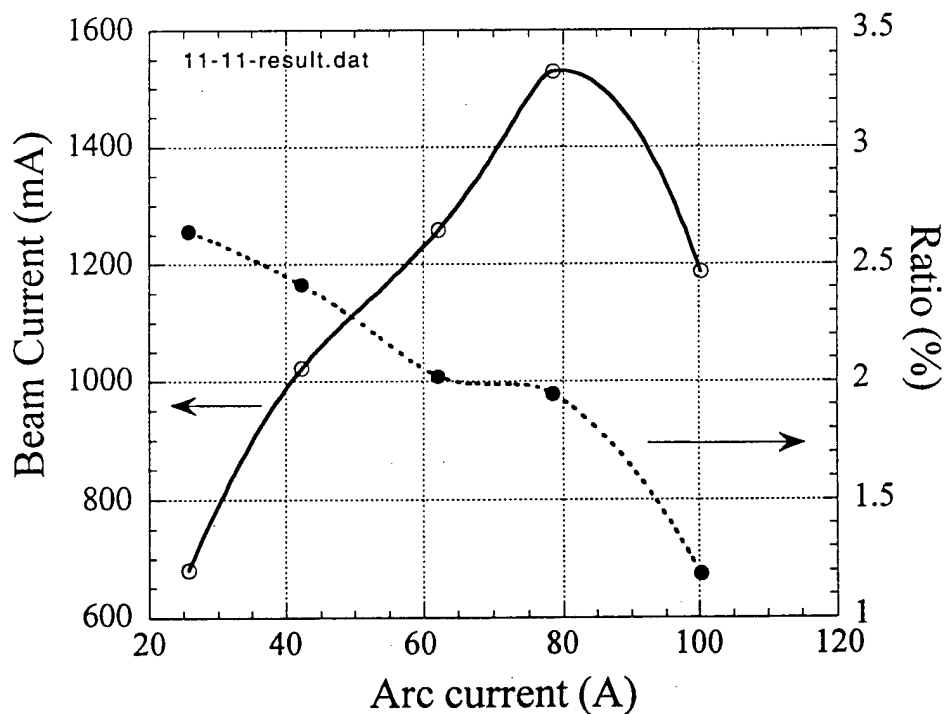


Figure 13 Total Bi beam current (dotted line) and the ratio of the beam current to the arc current vs. the arc discharge current (solid line). At higher arc currents, the beam current was lower. This will not be the case when properly designed extraction grids are used.

AC

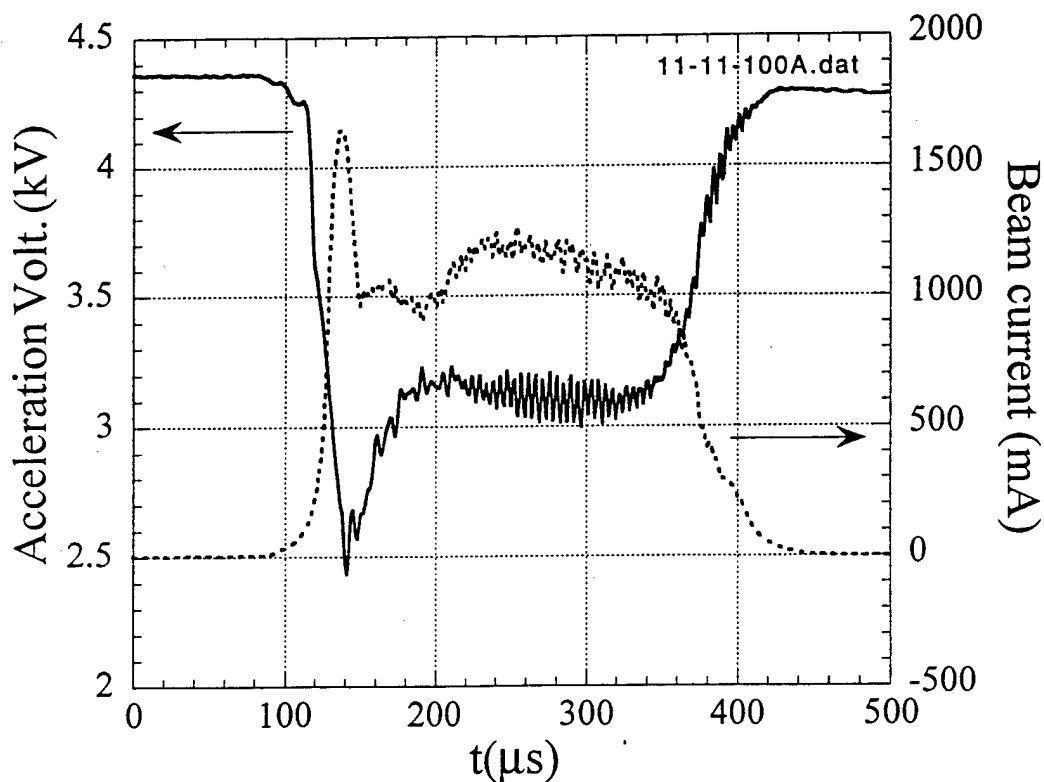


Figure 14a The Bi ion beam current (dotted line) and the net acceleration voltage (solid line) vs. time. The discharge current was ≈ 100 A.

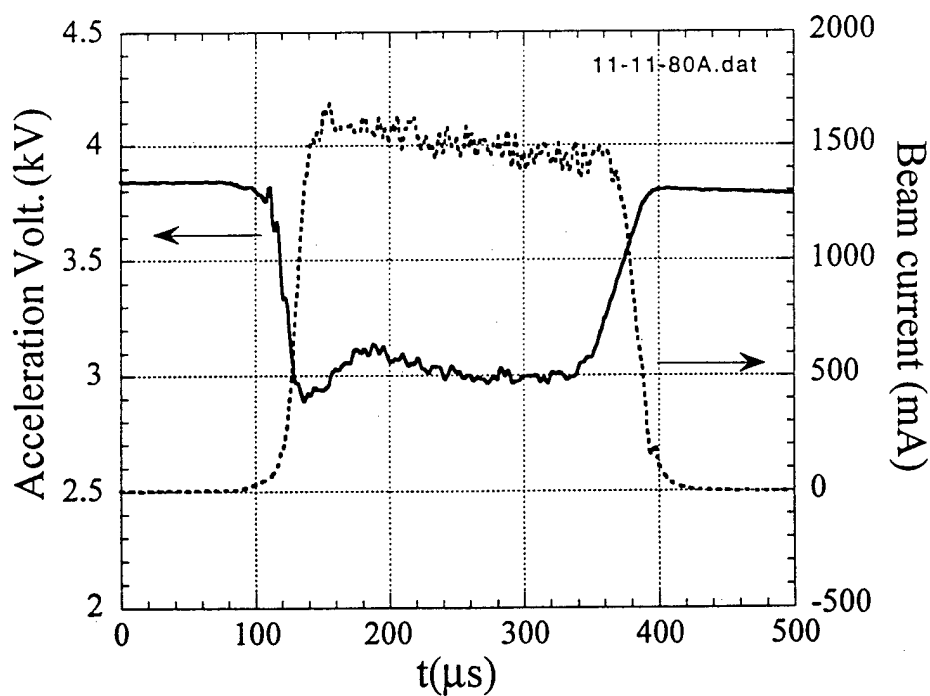


Figure 14b The Bi ion beam current (dotted line) and the net acceleration voltage (solid line) vs. time. The discharge current was ≈ 80 A.

AC

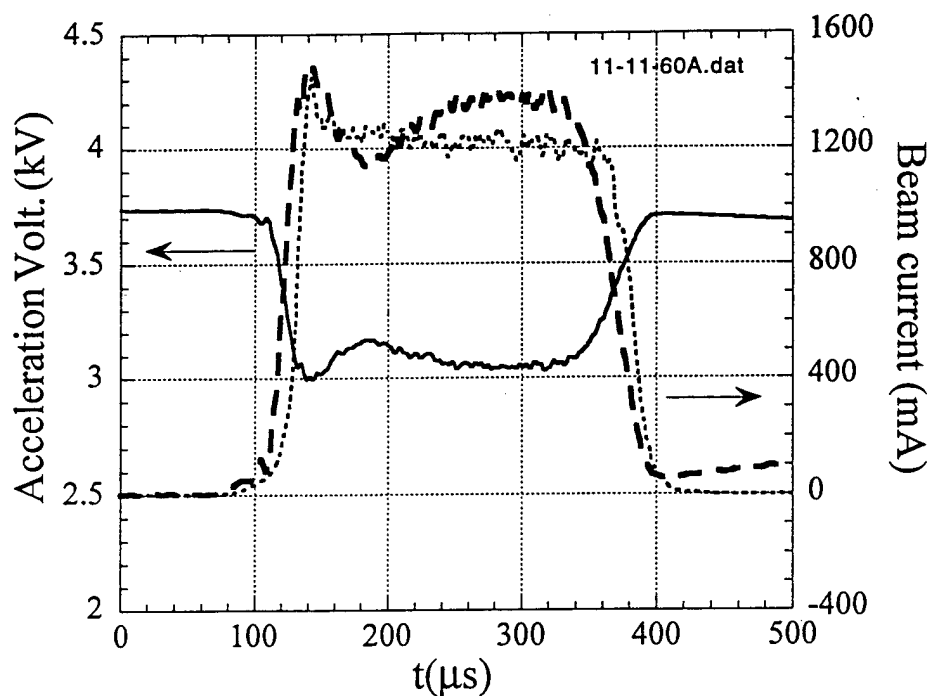


Figure 14c The Bi ion beam current (dotted line) and the net acceleration voltage (solid line) vs. time. The thick dashed line is the beam current derived from the acceleration voltage pulse, which agrees with the downstream Faraday cup measurements. The discharge current was ≈ 60 A.

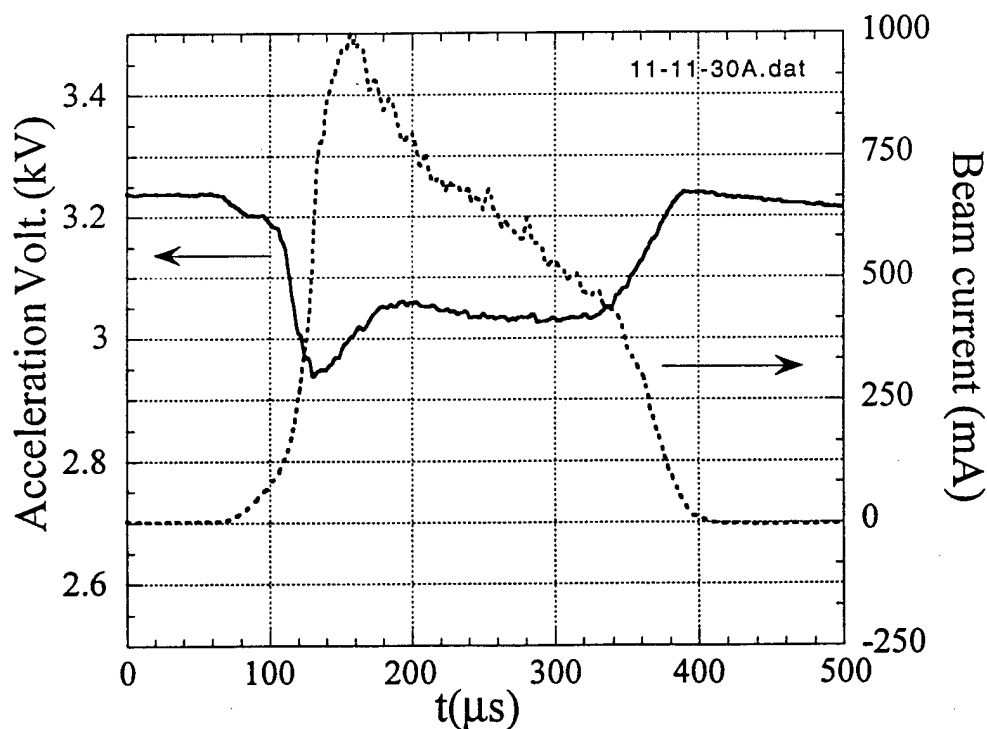


Figure 14d The Bi ion beam current (dotted line) and the net acceleration voltage (solid line) vs. time. The discharge current was ≈ 20 A.

AC

From the time-of-flight measurements, we found that most of the ions were in 1+ charge state and the ion streaming velocity matches the acceleration voltage. With a 3 kV acceleration voltage, the measured Bi ion velocity is $\approx 5 \times 10^4$ m/s. The ≤ 50 mrad. beam divergence was negligibly small. Knowing the beam current, charge state, its divergence and the ion velocity, the thrust level can be derived from,

$$\text{Thrust(N)} = \frac{m}{Ze} v I \alpha = 1.04 \times 10^8 \frac{\text{A}}{Z} v(\text{m/s}) I(\text{A}) \alpha \quad (2)$$

where $A(\approx 209)$ is the ion mass in atomic units, $Z(\approx 1.1)$ is the ion charge state, v is the ion streaming velocity and I is the ion beam current. α is the factor related to the beam divergence and is ≈ 1 when the divergence angle is small. Bi ion beams ≈ 1.3 A/3 kV were produced at arc current levels of ≈ 60 A, which imply a thrust level of 0.13 N. The total beam energy was derived by integrating the product of the beam current and acceleration voltage. Figure 15 shows the arc energy, beam energy and the energy efficiency of the VAIT as a function of the arc current. The energy efficiency, defined as the beam energy/(beam energy + arc energy), seems to decrease at the higher arc current levels. At 20-80A, it was about 80%. The goals of the Phase I were to produce a beam with an energy efficiency of $\approx 80\%$ and a divergence angle of ≤ 0.1 rad. Both goals have been achieved.

This is the most important milestone that we have achieved in the Phase-I project.

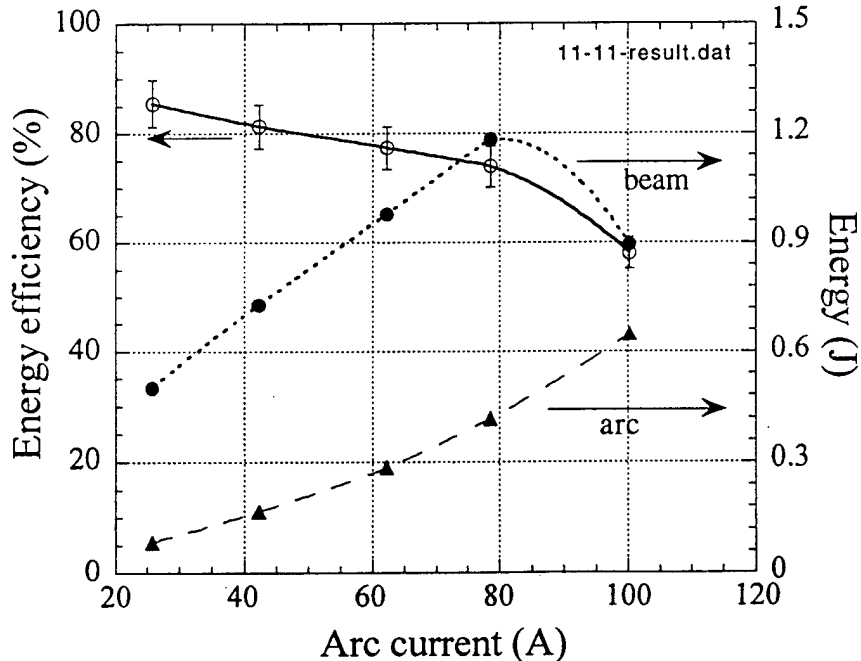


Figure 15 The energy of the Bi ion beam (solid dots) and the arc discharge (solid triangles) vs. the arc current. Also, shown is the energy efficiency of the thruster (open circles). For arc currents less than 80A, the efficiency is about 80%. At higher arc currents, the efficiency is lower due to the un-matched extraction grids.

3.2.3 Results from the two-grid acceleration system

The Bi ion beam experiments also carried out with a two-grid acceleration system, where the ground grid was removed. The two-grid system allowed an easy alignment of the grids and less restriction of the matching conditions between the grids and the nearby plasmas. The charge states of the beams remained the same as with the three-grid system since it is determined by the arc production. Figure 16 shows the typical beam current profile at an arc current of 80A. The ≈ 12 cm beam diameter was slightly larger than that from the three-grid system. The estimated divergence of the beam is about 80 mrad. Integrating the measured beam profiles, the total ion currents were obtained. Figure 17 shows the arc discharge and the total ion currents. Figure 18 shows the net acceleration voltage and the total beam current. The arc and beam current waveforms were very similar. For a 80 A arc discharge, the total beam current was as high as 2.8A. This ion current level is close to the saturated current of ≈ 4.2 A. Farther increasing the arc current caused electrical breakdown between the grids and the beam was not stable. Such breakdown might be prevented if a charge neutralizer were used instead of background gas. This needs investigation in future. Figure 19 shows the ratio of the beam current to the arc with the two-grid system. Also shown in Fig. 19 are the total beam current extracted from the two- and three-grids acceleration system. At low arc currents (≤ 40 A), both systems extracted more or less the same ion currents. When the arc current were high (≥ 60 A), more ion beams were extracted with the two-grid system than that with the three-grid system. In principle, the three-grid system should be able to extract more or less same amount of the ions with proper geometry of the grids, which requires comprehensive modeling. Figure 20 shows the measured energy in the arc discharge and the beam. From these measurements, the energy efficiency of the VAIT is about 80% as shown in Fig. 20.

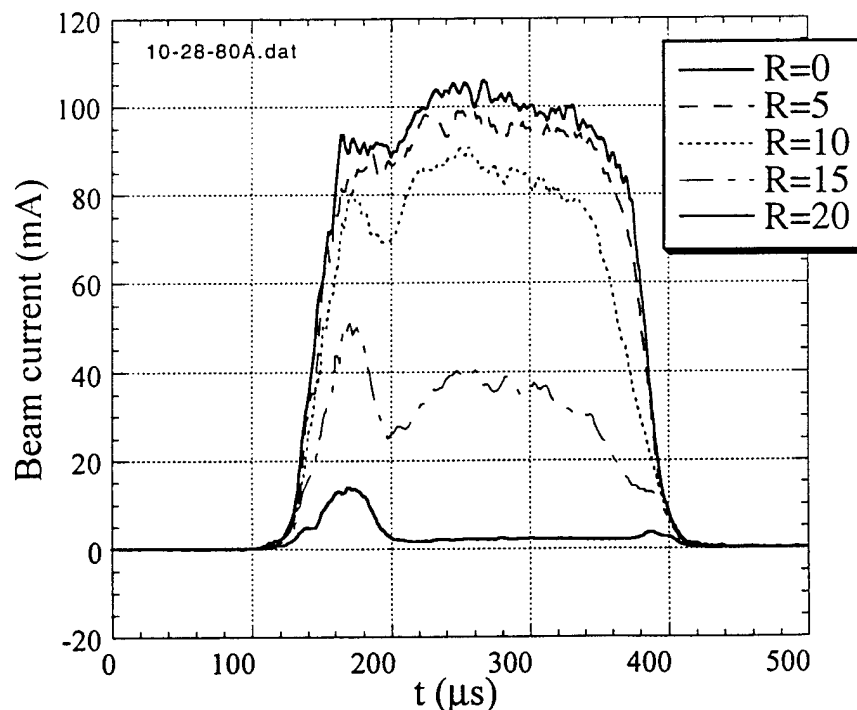


Figure 16 Measured Bi ion beam current at several radial positions with a 80 A arc discharge. The beam diameter was ≈ 12 cm.

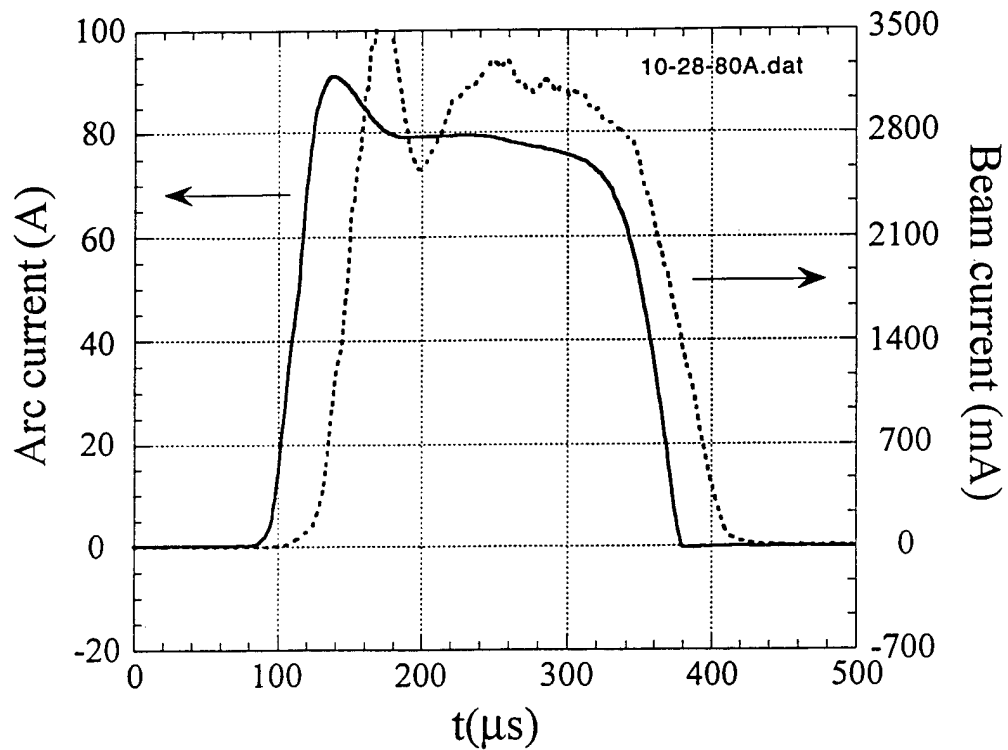


Figure 17 Bi arc discharge current (solid line) and total beam current (dotted line) vs. time.

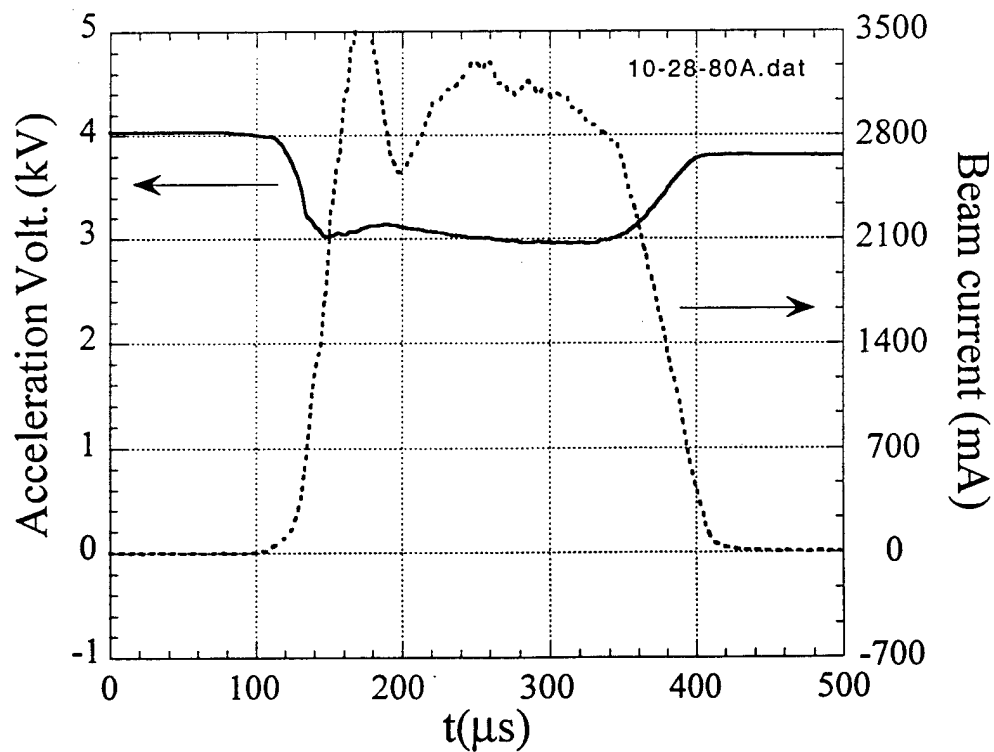


Figure 18 The Bi ion beam current (dotted line) and the net acceleration voltage (solid line) vs. time. The discharge current was ≈ 80 A.

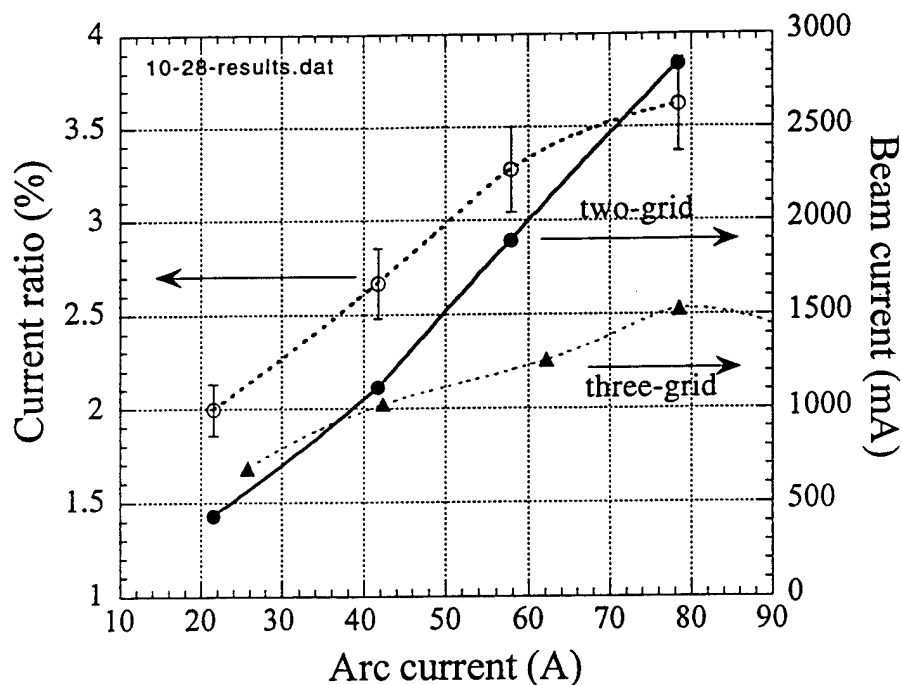


Figure 19 The ratio of the beam current to the arc current vs. the arc discharge current (open circles). Also shown is the measured total Bi ion beam current with the two-grid (solid dots) and with the three-grid (solid triangles) acceleration system.

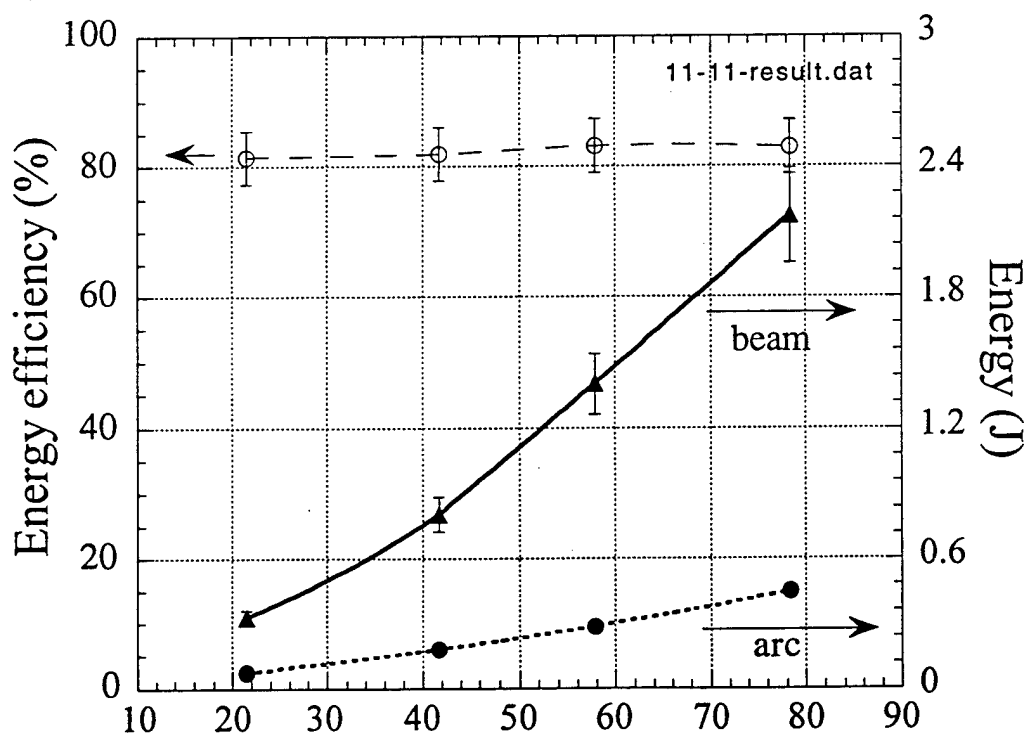


Figure 20 The energy of the Bi ion beam (solid triangles) and the arc discharge (solid dots) vs. the arc current. Also, shown is the energy efficiency of the thruster (open circles). The efficiency is about 80%.

AC

In summary, we have accomplished all of the objectives of the Phase-I vacuum arc ion thruster feasibility study. We have achieved the following milestones:

1. Produced a stable arc plasma at a 60 A/15 V power level;
2. Demonstrated that most ions were in 1+ charge state;
3. Measured the beam divergence to be <0.1 rad;
4. Measured the energy efficiency of the VAIT to be $\approx 80\%$.

The vacuum arc ion thruster produced up to 3 A Bi ion beams with ≈ 12 cm diameter acceleration grids. The measured $\approx 80\%$ efficiency of the vacuum arc ion thruster is comparable to the present Xenon ion thruster. Since the vacuum arc ion thruster is operated in pulsed mode, it is very easy to meet the input power limitation by adjusting the pulse width or repetition rates. Preliminary data analysis indicates that the vacuum arc ion thruster (VAIT), when fully developed by the Phase-II project, can be a good candidate for USAF space propulsion applications.

4. Key issues of the vacuum arc ion source for space propulsion applications

There are several issues to be addressed for the proposed vacuum arc ion thruster. These are: mission requirements, optimization of the arc discharge, cathode erosion rates, ion charge states, beam neutralization, and the lifetime of the source. All of these issues are discussed below:

1) Optimization of the arc plasma

The most important parameter of a thruster is its energy efficiency. The energy efficiency of the vacuum arc ion source is determined through many steps from total metal plasma generated by the arc to plasma transported to the beam formation electrodes, to the energetic ion beam extracted. A well-established basic feature of the vacuum arc discharge is the relationship between the metal ion flux that is generated at the cathode spots and the current that drives the arc [19-21]. The arc current is driven externally and in the arc itself is composed of both an electron component and an ion component; the "plasma ion current" is that part of the plasma flux generated at the cathode that is in the form of metal ions. It has been found that over a wide range of conditions the plasma ion current is a constant fraction of the arc current, $I_{\text{beam}} = \epsilon I_{\text{arc}}$, where ϵ is in the range 0.06 - 0.12. Thus the electrical efficiency of the vacuum arc, the ratio of available metal ion plasma current to arc current, is high, about 10%. The voltage drop of the arc discharge is typically 20 volts and varies according to the cathode metal used. If the ion current is 10% of the arc current, it takes ≈ 200 eV energy to produce an ion in the arc. In an ideal case, the energy efficiency could be $\approx 94\%$ when the ions in the discharge are propagated, accelerated and extracted at 3 kV without losses. For the space propulsion applications, the upper limit of the ion exhaust velocity (≈ 50 km/s) is restricted by the thrust/power ratio. Heavy elements are desired as the propellant since they have low thrust/beam current ratio and high acceleration voltage, which offers longer source life time and higher beam current density. Bismuth is the heaviest stable metal element. Due to its radioactivity and the possibility of spacecraft contamination, Uranium ($A \approx 238$) may not be acceptable as a propellant.

AC

With proper anode-cathode electrode geometry, most of the arc plasma flux can be directed towards the beam formation electrodes. An external magnetic field may also help plasma transport. The energy efficiency of the vacuum arc ion thruster can be high. In the Phase-I experiments, a ≈ 1.3 A, 3 kV Bi ion beam was extracted at a 60 A, 15 V arc discharge level, which implies that the energy efficiency of the source is $\approx 80\%$. Further increase of the extracted ion beam current to 6-10% of the arc current, thus $>90\%$ energy efficiency, is possible by optimizing the anode-cathode geometry.

The energy efficiency of the source strongly depends on the discharge voltage drop, although heavy elements offer some advantages. The arc voltage is mainly the sum of the plasma and electrode sheath voltage drops. The plasma Ohmic resistance is about 0.1Ω and can be reduced by increasing the cross section of the plasma. The electrode sheath voltage is a function of the product of the melting temperature and thermal-conductivity of the elements. Therefore, it is worth investigating other elements such as Al ($A=26$), Cu ($A=64$), Gd ($A=159$), Yb ($A=173$), W ($A=183$), and Pb ($A=207$). If the source can be operated efficiently with a wide range of elements, it provides more flexibility. For example, to maintain a fixed thrust level, only the propellant (cathode) is changed according to the available power. Vacuum arc ion sources with multiple cathodes (up to 16) have been developed and are routinely used at LBNL, where a cathode can be changed without breaking vacuum.[11]

To produce a suitable plasma source for ion thrusters, attention needs to be paid to the plasma parameters. The plasma density profile near the acceleration grid affects the beam current. Typically, the extraction grids used are uniformly spaced, and a uniform plasma density is preferred. Figure 15 shows ion beam current waveforms for several arc current levels in our earlier DOE Heavy Ion Fusion source development experiments.[5]

When the arc current was low, the beam current had a very slow rise-time. Since the plasma density was too low near the extraction grids, less ions were available for acceleration and the beam current was lower in amplitude. Increasing the arc current, the beam current waveform began to resemble that of the arc current. At 280 A arc current, the beam and arc current pulse shapes were similar to each other. At a higher arc current (~ 350 A), the beam current reached more-or-less the same peak in time as for the case of 280 A arc current. But it did not stay at that level afterward. Instead, the beam current decreased and then came up again. There was a dip, not a flat-top, in the beam current. When the arc current is low, there are few ions available to be extracted and the beam current is low. At the optimal conditions (perveance match) the beam divergence is minimum and the downstream beam current is maximum. For high plasma density, although there are many ions potentially available for extraction, the beam optics are poor and the net effect is that less beam current reaches the target. Thus it often occurs that the beam current maximizes during the rise and fall of the arc current (plasma density) with a decrease in between, as the optimal plasma density is obtained and passed through rapidly. The three measured beam current waveforms of Fig. 21 show this effect very clearly. Therefore, a more uniform plasma will provide a perveance match condition over a larger portion of the extraction grids area to make the system more compact.

To deliver more plasma to the acceleration grids and have a uniform plasma density profile, several arc anode-cathode configurations will be designed and tested. Beside these, effects

AC

of a coaxial magnetic field will also be investigated. A few hundred Gauss co-axial magnetic field may help duct the plasma plume in the forward direction. This B-field may also enable us to produce a uniform plasma density near the acceleration grids as we found in our earlier vacuum arc centrifuge-isotope separation project[22].

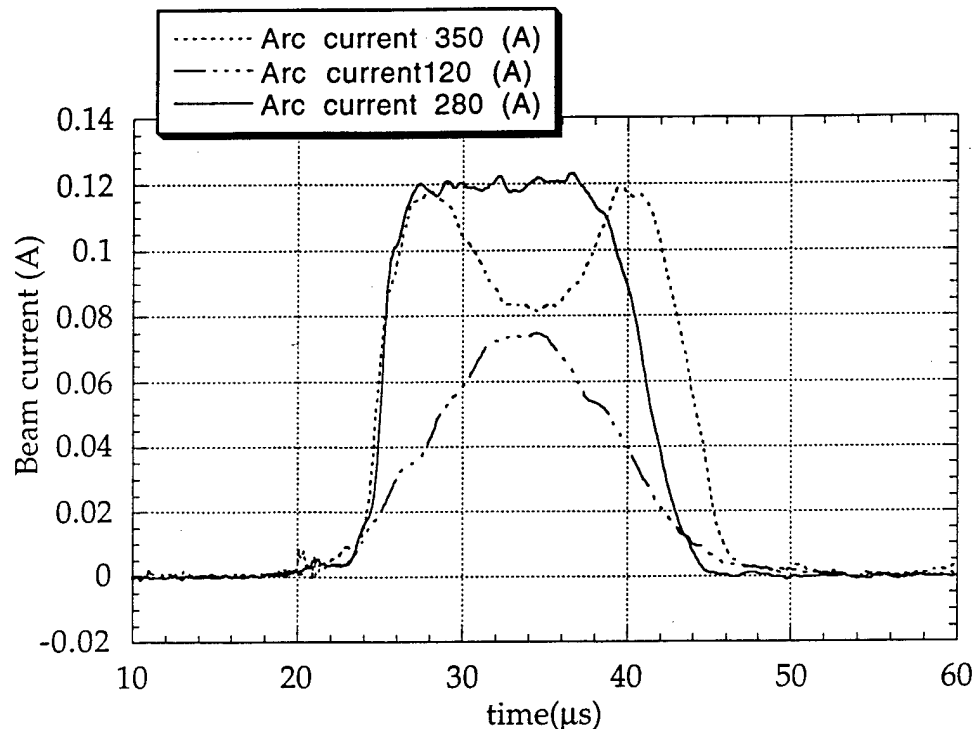


Figure 21 Typical beam current waveforms at several arc current levels.

To monitor the plasma density profile, several methods will be used. Witness plates will be inserted into the plasma column and ions will be deposited on the plates as thin metal films. Such methods has been successfully used for arc plasmas.[23] Scanning the thickness of these metal films gives us time integrated information of the ion flux and density profiles. Electrical probes such as Faraday cups and Langmuir probes will also be used to measure the plasma conditions such as temperature and ion current in the arc.[24]

2) Cathode Erosion rates

The cathode erosion rate is an important parameter for the proposed vacuum arc ion thruster. It relates to the mass utilization efficiency of the source. The relationship between the mass evolved from the cathode and the arc parameters has been investigated by AASC and PAG/LBNL in prior work and by other workers [19,25-27]. At the cathode spots, cathode material is converted into metal plasma, neutral gas, and solid "macroparticles". The macroparticles are metallic globules that are ejected from the cathode in the molten state and then rapidly solidify. They are typically of diameter in the range 0.1 - 10 microns. For many cases, especially the higher melting point cathode materials, the macroparticle content of the metallic ion beam produced by a vacuum arc ion source is small and is not a concern. If one neglects the macroparticles or limits consideration to those cases for which the macroparticle component of

the evolved flux is not great, the mass of the plasma generated by the vacuum arc is of order several tens of micrograms per Coulomb of arc current, where the precise value depends primarily on the metal used. By measuring the cathode erosion rates and ion flux in the arc plasma and the extracted ion beam, the cathode (propellant) mass utilization of the ion thruster can be determined.

Macroparticle generation also plays a major role in determining the overall plasma conversion efficiency. Neglecting the loss, the mass flux from the cathode is equal to that in the extracted beam, i.e.

$$M = I_{\text{arc}}/R_e = \frac{m}{e} I_{\text{beam}} \quad (3)$$

where R_e is the cathode erosion rate, m and e are the ion mass and charge, respectively. The efficiency of the source is given by,

$$\eta = \frac{V_{\text{beam}} I_{\text{beam}}}{V_{\text{beam}} I_{\text{beam}} + V_{\text{rc}} I_{\text{arc}}} = \frac{1}{1 + (2V_{\text{arc}})/\left(v^2 R_e\right)} \quad (4)$$

where v is the velocity of the extracted ion, which is related to the acceleration voltage, V_{beam} , as $eV_{\text{beam}} = 0.5 mv^2$. It is clear that higher specific impulses (or ion velocity) and erosion rates give higher efficiency. But there is a certain narrow range of specific impulses for a specified mission. Therefore, elements with high erosion rates and low arc voltage drops will be most attractive for the cathode. In the Phase-I work, the Bi cathode voltage drop was about 15 V and ions were accelerated to a velocity of 50 km/s. With the measured efficiency of 80%, this implies that the erosion rate was about 48 $\mu\text{g/C}$, which is comparable to the typical $\sim 50 \mu\text{g/C}$ ranges for arc cathodes reported by others.[19,25-27]

For high efficiency of conversion of cathode mass into useable plasma it is necessary that the macroparticle fraction be small. PAG/LBNL have developed a method for measurement of this feature of vacuum arc behavior, and have so characterized a range of cathode materials [27]. The plasma conversion efficiency of the cathode materials will be measured over a wide range of the source operation conditions, using PAG/LBNL techniques.

3) The lifetime of the source.

The lifetime of ion thrusters is of the order of 2000 to 8000 hours over 5-10 years as required by various mission applications. It is not realistic for us to attempt a lifetime evaluation in the Phase-II project. That is what we hope will happen at Phillips Lab. following successful completion of our Phase-II development. Nevertheless, the Phase-II project can obtain useful data by performing very limited but relevant bursts. For example, if data are gathered at 111 Hz with 1 ms pulses (10% duty factor), the idea would be to run bursts of 1, 10, 100 seconds etc. and extrapolate the data to much longer times. In our project we will address the following critical issues when the ion source is operated in burst mode for such limited burst duration.

i. Deposition of arc plasma and sputtered material within the discharge chamber;

AC

- ii. Erosion of the arc discharge trigger;
 - iii. Deposition of conducting layers on the internal and external surface of isolators and insulators;
 - iv. Contamination of micro-particles and plasmas;
 - v. Acceleration grid erosion due to the ion bombardment.
- 4) Ion charge state

Above a certain threshold arc discharge current density, the beam from the source will contain not only single charged ions but also higher charge states. The presence of these ions gives rise to a need to correct the propellant utilization and thrust level. Therefore, the charge state distribution of the extracted ion beam will be monitored closely.

Charge state distributions (CSD) of ions generated by the metal vapor vacuum arc have been reported previously by PAG/LBNL [13,28,29] and also by several other workers [30-33]. The ion charge state spectrum is important fundamentally for an understanding of the physics of vacuum arc cathode spots, and for this reason, PAG/LBNL have studied the ion charge state distributions quite extensively. Ion spectra have been measured for a wide range of metallic cathode materials, including Li, C, Mg, Al, Si, Ca, Sc, Ti, V, Cr, Mn, Fe, Co, Ni, Cu, Zn, Ge, Sr, Y, Zr, Nb, Mo, Pd, Ag, Cd, In, Sn, Sb, Ba, La, Ce, Pr, Nd, Sm, Gd, Dy, Ho, Er, Tm, Yb, Hf, Ta, W, Ir, Pt, Au, Pb, Bi, Th and U [13,28]. The spectra produced by a range of compound and alloy cathode materials, including for example TiC, SiC, UC, PbS, brass, and stainless steel are also investigated[21].

The ion beam source can be viewed as a diagnostic for performing accurate and detailed characterization of the vacuum arc metal plasma ion composition. The charge state distribution of the extracted ion beam is measured using a time-of-flight (TOF) diagnostic [18]. In this method, a set of deflection plates is located in the beam path and biased so as to deflect the beam aside except for a short pulse of about 0.2 microseconds in length. This short beam pulse sample is drifted down a region of sufficient length (about 1 meter or less) to allow the different charge-to-mass (Q/A) components of the beam to separate out, since they have been accelerated through the same potential drop in the ion source extractor and thus have flight times proportional to $(Q/A)^{1/2}$. A detector, a well shielded Faraday cup with magnetic suppression of secondary electrons, at the end of the drift chamber, measures the arrival time of the different Q/A components of the beam. The beam is steered onto the detector by annular gating plates and the detector is prevented from viewing the intense visible light and UV generated by the vacuum arc by blocking the direct path with a metal plate which also serves as a beam current monitor. The detector measures the electrical current in the different charge states and provides a good measurement of the CSD of the extracted ion beam. The measured flight times for the various charge states can be well fitted by the calculated values, usually to better than the measurement uncertainty of about 1%.

An example of a typical charge state spectrum obtained is shown in Figure 22, where an oscillogram of a time-of-flight ion spectrum of a Gd plasma is shown.

AC

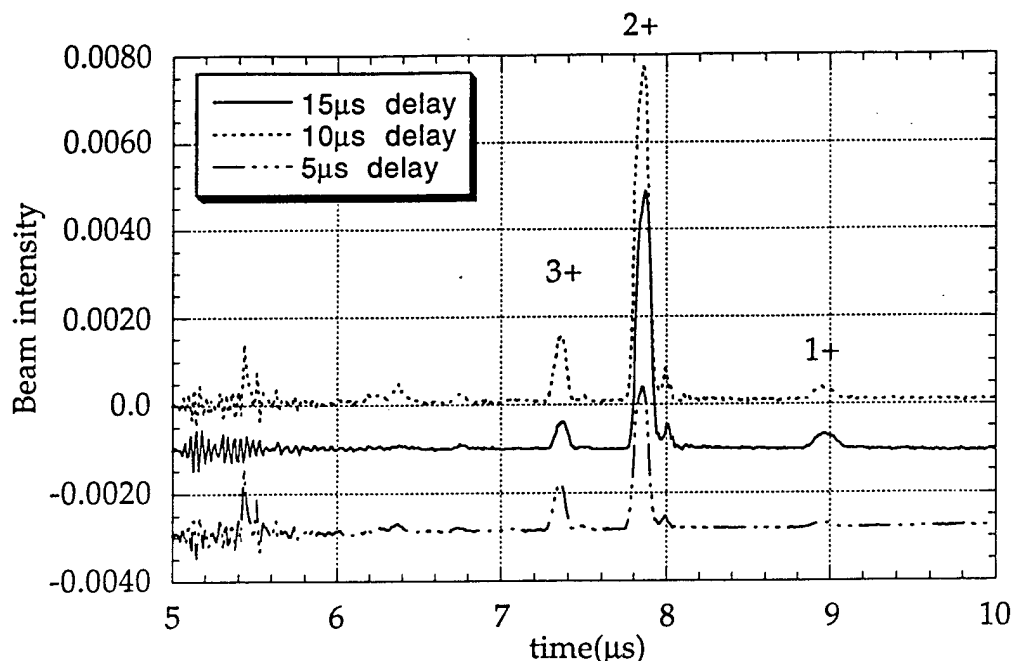


Fig. 22 Charge state distributions of a gadolinium ion beam at $t=5, 10$ and $15 \mu\text{s}$ after the beginning of the current. About 85% of ions are in the $2+$ charge state as measured at PAG/LBNL using TOF technique.

This signal is produced by the beam current into a Faraday cup, and is thus electrical current. For beams of multiply-charged ions the electrical current, I_{elec} , in the beam is not the same as the particle current, I_{part} , but $I_{\text{part}} = I_{\text{elec}}/Q$. It is important to keep this distinction in mind, including especially for thruster application where the electrical current might be measured but the particle current is important for estimating the thrust. The ions generated by the vacuum arc could be multiply-stripped with a mean charge state of from 1 to 3, depending on the particular metal species, and the charge state distribution can have components from $Q = 1+$ to $6+$; thus the ion energy is greater than the extraction voltage by this same factor. Lower boiling point metals tend to have lower mean charge state. The exact spectrum obtained depends on the arc operating conditions, including arc current, pulse duration, pulse repetition rate, among other things. For full characterization of the plasma generator used for the vacuum arc thruster, PAG/LBNL will carry out time-of-flight measurements under the anticipated operational conditions.

5) Beam neutralization

Neutralization of the ion beam is very important to allow the ion beam to propagate. The existing thermal electron beam neutralizer on xenon thrusters can be easily adapted for the vacuum arc ion thruster. But a pulsed e-beam source might be more suitable as our source will be operated in pulsed mode. Recent advances in long lifetime (~ 5000 hours) cold cathode e-beam sources for a flat panel display are potentially applicable. Recently AASC has co-operated with a group at UC Davis to develop a cold cathode e-beam source for a new type of high voltage, high

power diamond switch. The feasibility of the cold cathode e-beam source for ion beam neutralization will be studied and the latest results will be adopted if possible.

6) Mission requirements

Much of the work in demonstrating the feasibility of the Vacuum Arc Ion Source has been accomplished in Phase-I. Successful transition of this preliminary work into a commercial reality also requires a combined technical and mission-oriented system analysis.

Recent interest in the development of small satellite systems has prompted examination of alternatives to existing electric propulsion techniques. Space applications of electric propulsion include electrothermal thrusters in the form of resistojets and kilowatt-level arcjets, electromagnetic devices, represented by the pulsed plasma microthruster (PPT) and the various Hall thrusters (e.g., SPT-100), and electrostatic engines, such as the xenon ion propulsion system (XIPS), the UK-10 and the radiofrequency ion thrusters (RIT). All of these systems have a long history of development and, in many cases, corporate investment. The electrothermal engines and the PPT have substantial flight experience as on-board propulsion for station-keeping. The others may soon see actual application (vs. flight demonstration). To displace or supplement this technology with new devices or components is a challenge that requires efforts both in system analysis to find the appropriate entry point and in detailed technical examinations to understand physical behavior and scaling.

Development of ion sources for electrostatic thrusters has a very long history. At one time, for example, metals were the favored approach, in the form of contact-ionization of cesium and later in the electron-bombardment source using mercury. Concern for clogging of the porous tungsten plug, especially for restart, contributed to the rejection of cesium as a propellant; handling of alkali metals was also a factor. The field-emission thruster (FET) for very low impulse missions still uses cesium. Mercury achieved great success, including spaceflight demonstrations, but environmental issues led to its rejection as well. High thrust densities favor high values of mass-to-charge ratio, and a very strong desire for a single species of ion for chemical simplicity. Xenon, therefore, has become the propellant of choice for near earth missions; noble gases of lower molecular weight, such as argon and krypton, can serve higher specific impulse missions. The problem with a gaseous propellant arises because of the need for tanks, valves and other plumbing, the masses of which do not scale well for small satellite needs. Solid propellants can avoid this problem, requiring only a bit of ingenuity for propellant handling. The conversion of a solid into a collection of ions all of the same charge-state, however, can present a significant challenge. The Vacuum Arc Ion Source appears to have demonstrated capability for accomplishing such conversion with reasonable simplicity and efficiency. The nature of the source permits consideration of many candidate propellants. The electrical operation as a pulsed system also offers considerable flexibility for system design. In re-visiting the use of metallic propellants questions of mass utilization and subsequent distribution must be addressed. By introducing pulsed operation, different concerns for component lifetime (e.g., wear due to transients) trade against similar issues in steady state devices. System power-density improves by avoiding gas-handling. Solid propellants require only a bit of ingenuity for propellant handling. The conversion of a solid into a collection of ions all of the same charge-state must be sufficiently high to avoid significant degradation of the system specific impulse. (Mass

AC

removed from the cathode, but not ejected at high velocity, does not contribute positively to the performance of the thruster.) Subsequent acceleration to high energy certainly mitigates the energy cost per ion in the source, but involves limitations associated with the overall system and mission design. Trade-off for propellant type and electrical operation require understanding of source behavior in terms of propellant and energy efficiencies.

7) Environmental factors of the proposed vacuum arc ion thruster

The primary environmental factors are:

- i. Material sputtered from the extraction grids;
- ii. Efflux of neutral atoms and plasmas;
- iii. EMC Factors.

In a xenon thruster, about 85% materials sputtered from the grids are due to charge exchange. As fully ionized plasmas are produced in the vacuum arc ion thruster, the sputtering yield of the grids will be much lower. As reported in Ref. [34], the thickness of this deposition is of concern only close to the thruster after 5000 hours of operation.

Problems due to the efflux of the plasmas on a xenon ion thruster have not been reported. Contamination of space crafts by the plasmas due to the earth's magnetic field may not be a serious issue as a xenon plasma is much more reactive than metal arc plasmas. However, there are micro-particles in the arc discharge. Though these particles are almost as directional as the ion beam flux, a small flux of stray atoms is expected to reach the spacecraft. Condensation of this flux onto sensitive cold surfaces over long periods of time is a potential concern, although methods to alleviate the problem are available. The proposed cathode erosion measurements, discussed before, will enable us to estimate and/or reduce this efflux.

As reported in Ref. 34, the RF noise produced by a xenon ion thruster can be controlled at an acceptable level. Therefore, it is possible to minimize the electrical noise of the vacuum arc ion thruster to more or less the same level as xenon ion thruster.

8) Other Issues

One of the other issues is the thermal management of the thrusters. Present xenon ion thrusters are operated in steady-state with several thousand start/stop cycles. It has been demonstrated that by operating the xenon ion thruster at a power level much lower than that designed, the lifetime of the thrusters is extended.[35] Such derated power operation is eminently possible in a pulsed vacuum arc ion thruster. For a 4000 hours, 5 year mission, the average power is about 45 W, which can be achieved by operating a 4.5 kW/1 ms vacuum arc ion source at a repetition rate of 10 Hz.

References

AC

1. I. G. Brown, "Vacuum arc ion sources", Rev. Sci. Instrum. **65**, 3061 (1994). See also the accompanying papers in this issue by authors from many different laboratories around the world.
2. I. G. Brown, "Vacuum arc ion sources for particle accelerators and ion implantation", IEEE Trans. Plasma Sci. **21**, 537 (1993),
3. I. G. Brown, "The metal vapor vacuum arc ion source", in The Physics and Technology of Ion Sources, edited by I. G. Brown (Wiley, N.Y., 1989), p. 335.
4. I. G. Brown and X. Godechot, IEEE Trans. Plasma Sci., **PS-19** (1991) 713.
5. F. Liu, N. Qi, S. Gensler, R. R. Prasad, M. Krishnan and I. G. Brown, "A Vacuum Arc Ion Source for Heavy Ion Fusion", Rev. Sci. Instrum. **69**, 819 (1988).
6. I. G. Brown, J. E. Galvin, and R. A. MacGill, "High current metal ion source", Appl. Phys. Lett. **47**, 358 (1985).
7. T.S. Green, IEEE Trans. Nucl. Sci. **NS-23**, 918 (1976).
8. A. T. Forrester, *Large ion beams* (Jhon Wiley & Sons, New York, 1988).
9. G. Kanning, "Measured Performance of Water Vapor Jets for Space Vehicle Attitude Control Systems," NASA TN D-3561, NASA, Washington, 1966.
10. M. Wolff, A. J. Kelly, and R. G. Jahn, "A High Performance MPD Thruster," IEPC 84-32, Proc. of the 17th Intl. Electric Propulsion Conf., Tokyo, 1984.
11. R. L. Burton, S. G. Delmedico, M. J. Wilson, "High Efficiency Pulsed Plasma Thruster", US Patent Application Serial No. 08/832,293, April 3, 1997.
12. D. L. Tilley and R. A. Spores, "Life Extension Strategies for Space Shuttle-deployed Small Satellites Using a Pulsed Plasma Thrusters," 32nd Joint Propulsion Conf., AIAA Paper 96-2730, Lake Buena Vista, FL July 1-3, 1996.
13. I. G. Brown, "Vacuum arc ion sources", Rev. Sci. Instrum. **65**, 3061 (1994). See also the accompanying papers in this issue by authors from many different laboratories around the world.
14. I. G. Brown, "Vacuum arc ion sources for particle accelerators and ion implantation", IEEE Trans. Plasma Sci. **21**, 537 (1993).
15. Juergen Mueller, "Thruster options for microspacecraft: A review and evaluation of existing hardware and emerging technologies," 3rd AIAA/ASME/SAE/ASEE Joint Propulsion Conf. and Exhibit, AIAA Paper 97-3058, June 6-9, 1997, Seattle, WA.
16. G. Kanning, "Measured Performance of Water Vapor Jets for Space Vehicle Attitude Control Systems," NASA TN D-3561, NASA, Washington, 1966.
17. M. Wolff, A. J. Kelly, and R. G. Jahn, "A High Performance MPD Thruster," IEPC 84-32, Proc. of the 17th Intl. Electric Propulsion Conf., Tokyo, 1984.
18. I. G. Brown, J. E. Galvin, R. A. MacGill and R. T. Wright, Rev. Sci. Instrum. **58**, 1589 (1987).
19. "Vacuum Arcs - Theory and Applications", edited by J. M. Lafferty (Wiley, New York, 1980).
20. C.W. Kimblin, J. Appl. Phys. **45**, 5235 (1974).
21. C. W. Kimblin, in Proc. 11th Int. Conf. Phenomena in Ionized Gases (Prague), 1973, p. 73.
22. N. Qi and M. Krishnan, "The high Separative Power Vacuum Arc Centrifuge", ANS Trans., p. 530, Isotope Production and Applications Embedded Topical, ANS Winter Meeting, Nov. 16-20, 1997, Albuquerque, New Mexico.
23. R.R. Prasad, Ph.D. thesis, Yale University, 1987.

24. I. H. Hutchinson, *Principles of Plasma Diagnostics* (Cambridge University Press, Cambridge, 1987).
25. R. R. Prasad, R. Consiglio and M. Krishnan, "Power Flow and Cathode Erosion in a Vacuum Arc Centrifuge," IEEE Trans. Plasma Sci. **PS-14**, 498 (1986).
26. C.W. Kimblin, J. Appl. Phys. **44**, 3074 (1973).
27. I. G. Brown and H. Shiraishi, IEEE Trans. Plasma Sci. **PS-18**, 170 (1990).
28. I. G. Brown and X. Godechot, IEEE Trans. Plasma Sci. **PS-19**, 713 (1991).
29. J. Sasaki and I. G. Brown, J. Appl. Phys. **66**, 5198 (1989).
30. A.A. Plyutto, V.N. Ryzhkov and A.T. Kapin, Sov. Phys. JETP **20**, 328 (1965).
31. W.D. Davis and H.C. Miller, J. Appl. Phys. **40**, 2212 (1969).
32. V.M. Lunev, V.G. Padalka and V.M. Khoroshikh, Sov. Phys. Tech. Phys. **22**, 858 (1977).
33. M. J. Patterson and J. E. Foster, "Performance and optimization of a 'derated' ion thruster for auxiliary propulsion", 27th Joint Propulsion Conf., June 24-27, 1991, Sacramento, CA, AIAA-91-2350
34. D. G. Fearn, "Factors influence the degradation of the UK-10 ion thruster system with a spacecraft", 19th Intl. Elect. Propulsion Conf., Colorado Spring, May 11-13, 1987, AIAA 87-1004.
35. M. J. Patterson and J. E. Foster, "Performance and optimization of a 'derated' ion thruster for auxiliary propulsion", 27th Joint Propulsion Conf., June 24-27, 1991, Sacramento, CA, AIAA-91-2350